KfK 4104
Juni 1987

Physical and Chemical Behavior of LWR Fuel Elements up to very High Temperatures

S. Hagen, P. Hofmann
Hauptabteilung Ingenieurtechnik
Institut für Material- und Festkörperforschung
Projekt Nukleare Sicherheit

Kernforschungszentrum Karlsruhe

KERNFORSCHUNGSZENTRUM KARLSRUHE
HAUPTABTEILUNG INGENIEURTECHNIK
INSTITUT FÜR MATERIAL- UND FESTKÖRPERFORSCHUNG
PROJEKT NUKLEARE SICHERHEIT

KfK 4104

Physical and chemical Behavior of LWR Fuel Elements up to very high temperatures

S. Hagen, P. Hofmann

KERNFORSCHUNGSZENTRUM KARLSRUHE GMBH, KARLSRUHE

Als Manuskript vervielfältigt
Für diesen Bericht behalten wir uns alle Rechte vor

Kernforschungszentrum Karlsruhe GmbH
Postfach 3640, 7500 Karlsruhe 1

ISSN 0303-4003

Summary

Chemical interactions between UO_2 fuel and Zircaloy cladding up to 2350°C are described. UO_2/Zircaloy single effects tests have been performed with short LWR fuel rod segments in inert gas and under oxidizing conditions. The reaction kinetics of molten Zircaloy cladding with solid UO_2 fuel has been investigated with UO_2 crucibles containing molten Zircaloy. The UO_2/Zircaloy reactions obey parabolic rate laws. The oxygen uptake by solid Zircaloy due to chemical interaction with UO_2 occurs nearly as quickly as that from the reaction with steam or oxygen.

To study the competing effects of the external and internal cladding oxidation under realistic boundary conditions and the influence of the uncontrolled temperature escalation due to the exothermic steam/Zircaloy reaction on the maximum cladding temperature, single rod and bundle experiments have been performed. Electrically heated fuel rod simulators, including absorber rod material (Ag, In, Cd alloy for PWR or B_4C for BWR), guide tubes and grid spacers are used.

The maximum measured cladding temperature during the temperature escalation was about 2200°C. The failure temperature of the Ag/In/Cd-absorber rods and the extent of bundle damage depends on the guide tube material (Zircaloy or stainless steel) and varies between 1200 and 1350°C. In boron carbide absorber rods the cladding starts to be liquefied due to interactions between boron carbide and stainless steel at about 1200°C. The liquid reaction product may then react with Zircaloy. The molten materials and liquid reaction products can relocate and form large coherent lumps on solidification, which may result in complete blockage of the fuel rod bundle cross section.

In the future, 7x7 bundle experiments of 2 m overall length will be performed in the new CORA facility to study, in addition, the influence of quenching on fuel rod integrity.

Physikalisches und chemisches Verhalten von LWR Brennelementen bis zu sehr hohen Temperaturen.

Kurzfassung

Die chemischen Wechselwirkungen zwischen UO_2-Brennstoff und Zircaloy-Hülle im Temperaturbereich bis über 2000°C werden beschrieben. UO_2/Zircaloy Einzeleffekt-Untersuchungen wurden mit kurzen LWR Brennstababschnitten in Inertgas und unter oxidierenden Bedingungen durchgeführt. Die Reaktionskinitik geschmolzener Zircaloy-Hüllrohre mit UO_2-Brennstoff wurde an UO_2 Tiegeln untersucht, die flüssiges Zircaloy enthielten. Die UO_2/Zircaloy Reaktionen zeigen eine parabolische Zeitabhängigkeit. Die Sauerstoffaufnahme im festen Zircaloy infolge der chemischen Wechselwirkung mit UO_2 geschieht nahezu genau so schnell wie bei der Reaktion mit Dampf oder Sauerstoff.

Für die Untersuchung der konkurrierenden Effekte der Wechselwirkung zwischen Hüllrohr und UO_2 und der Oxidation im Dampf unter realistischen Randbedingugnen (Temperatureskalation), wurden Einzelstab- und Bündelexperimente durchgeführt. Hierfür wurden elektrisch beheizte Brennstabsimulatoren einschließlich Absorberstäbe (AgInCd für BWR oder B_4C für SWR), Führungsrohre und Abstandshalter verwendet.

Die maximal gemessenen Temperaturen bei der Temperatureskalation betrug ca. 2200°C. Die Versagenstemperatur der AgInCd-Absorberstäbe hängt vom Führungsrohrmaterial (Zircaloy oder Edelstahl) ab, und variiert zwischen 1200°C und 1350°C. Bei Borcarbid-Absorberstäben beginnt die Hülle bei ca. 1200°C durch Wechselwirkung zwischen dem B_4C und dem Edelstahl zu schmelzen. Die flüssigen Reaktionsprodukte können dann mit dem Zircaloy reagieren. Die geschmolzenen Materialien können beim Erstarren zusammenhängende Klumpen bilden, die in weitgehenden Blockaden des Bündels resultieren.

In der Zukunft werden in der CORA-Anlage 7x7 Bündelexperimente mit 2 m langen Bündeln durchgeführt um zusätzlich den Einfluß des Wiederflutens auf das Schandensverhalten des Bündels zu untersuchen.

Content

1. Introduction

In a severe fuel damage (SFD) accident, the fuel and the cladding may reach temperatures up to the melting point of UO_2. However, the temperature transient can be stopped before an uncontrolled core meltdown occurs. With increasing fuel and cladding temperatures, fuel rod damage will occur in the core in a variety of forms. A point of special concern is the formation of liquid phases, which may relocate, solidify, and form potential coolant channel blockages.

Since Zircaloy (Zry) is thermodynamically unstable with respect to steam and UO_2, chemical interactions will take place which become significant at temperatures above 1200°C and which have an influence on the chemical and mechanical integrity of the fuel rods and bundles. Zr, U and oxygen are not the only elements in the fuel rod bundles and the reactor core. Fe, Cr, and Ni of the structural materials as well as a (Ag,In,Cd)alloy or B_4C of the absorber rods of PWR or BWR are also present, causing additional complex chemical interactions. Especially the low-temperature melting of the (Ag, In, Cd) absorber material (about 800°C) may significantly influence the damage mechanisms of the bundles, the formation of blockages, the release of fission products and the aerosol generation.

The SFD experiments performed by the Nuclear Safety Project of the Karlsruhe Nuclear Research Center have served to investigate the most important physical and chemical phenomena of fuel element behavior beyond the current design limit (large-break LOCA, 1200°C) up to core meltdown phenomena. The experiment results will be used for the assessment of SFD codes and their capability to describe integral fuel element behavior.

This paper describes the results of out-of-pile reaction experiments with LWR fuel rod sections and electrically heated fuel rod simulators up to 2200°C under oxidizing conditions. In addition, the dissolution of solid UO_2 by molten Zircaloy cladding was studied in the temperature range of 1900-2300°C.

2. UO_2/Zircaloy Chemical Interactions

2.1 UO_2/Solid Zircaloy Reaction Experiments

The out-of-pile UO_2/Zry reaction experiments were performed in Ar or an (Ar + 25 vol.% O_2) gas mixture in the high temperature/high pressure autoclave apparatus MONA /1,2,3,6,8/. Short cladding tube specimens filled with stoichiometric high-density UO_2 pellets were used in the tests. The specimens were 100 mm long with an outside diameter of 10.75 mm and a wall thickness of 0.72 mm. The specimen was contained in a high-pressure vessel and inductively heated , with the cladding acting as susceptor. The experimental procedure is described in detail in /2,3/. The maximum cladding temperature was 1700°C in isothermal experiments and the annealing times varied between 1 and 150 min. The temperature transient experiments were performed with equal heating and cooling rates of 0.25, 1, 5, and 10 K/s. The maximum temperature varied between 1000 and 2000°C. The holding time at the maximum temperature was 10 s. At temperatures above the melting point of Zircaloy ($\approx$ 1760°C) a part of the cladding melted (unreacted β-Zr). However, due to the ZrO_2 shell forming on the outside surface of the cladding, the molten material remaind at place. On the other hand, the melting point of Zircaloy is shifted from about 1760 to 1960°C [melting point of oxygen-saturated α-Zr(O)] as a result of oxygen uptake. The external overpressure could be varied between 1 and 200 bar, but was about 40 bar in most of the experiments.

The results of the UO_2/solid Zry reaction experiments under isothermal and transient temperature conditions have been extensively described in /1,2,3,7,8,15/. The results show that due to oxygen uptake by the Zry cladding from reaction with gaseous oxygen or steam on the outside and from reaction with UO_2 on the inside oxygen stabilized α-Zr(O) phases, ZrO_2 and a metallic (U, Zr) alloy form. The sequence of the various phases, starting from the inside surface, is for isothermal and transient temperature experiments at all temperatures:

$[UO_2+U]\rightarrow[\alpha\text{-}Zr(O)_a+(U,Zr)^*]\rightarrow[U,Zr]\text{alloy}\rightarrow\alpha\text{-}Zr(O)_b\rightarrow\beta\text{-}Zry\rightarrow\alpha\text{-}Zr(O)_c\rightarrow ZrO_2.$

Figure 1 shows the sequence of external and internal interaction layers. The α-$Zr(O)_{a,b}$ layers forming on the inside of the cladding and the α-$Zr(O)_c$ layer forming on the outside of the cladding grow at roughly the same rates. Moreover, due to the elevated oxygen potential (oxygen partial pressure) of the gas mixture or steam compared to stoichiometric UO_2, a ZrO_2 layer also forms on the external cladding surface. The thicknesses of the various interaction layers determined metallographically as a function of temperature and time are plotted versus the square root of time in Figure 2 at 1020, 1100, 1200, and 1300°C. Initially, the growth of the reaction layers, obey parabolic rate laws. However, since the wall thickness of the cladding is small (0.72 mm), the tubing must be considered as a finite system. For this reason, the external and the internal oxygen uptake influence each other and an accelerated growth of the reaction layers is observed at longer reaction times, especially after the β-phase has disappeared. The thicknesses of the reaction layers in the transient temperature experiments are documented in /6,8/.

With increasing time the β-phase of the cladding disappears due to oxygen uptake and transformation into α-Zr(O). The growth of the various layers as functions of temperature and time and the inrease in fuel rod diameter due to the formation of ZrO_2 are evident. The time required to completely convert the β-Zry region in the center of the cladding to α-Zr(O) is highly temperature dependent. After the disappearance of the β-phase, the oxidized cladding tube is completely embrittled and is no longer mechanically stable. The slightest force exerted during cooling or subsequent handling causes the fuel rod sections to

---

* The (U,Zr) alloy within the α-$Zr(O)_a$ layer is concentrated mainly at the grain boundaries, but also within the matrix.

break apart. Since embrittlement of the cladding occurs as a result of the formation of oxygen-stabilized α-Zr(O), the internal oxidation makes approximately the same contribution as the external oxidation. For this reason, embrittlement of the cladding occurs about four times faster than by one-sided oxidation alone. The time to embrittlement is about 3 minutes for double-sided oxidation of the cladding at 1400°C (Figure 3). At 1020°C, the cladding is still ductile even after the longest reaction time examined of 150 min. Figure 3 indicates also the conditions for which embrittlement of the cladding must be anticipated in temperature transient experiment (upper scale). The slower the heating and cooling rates, the lower the temperature at which the ductile β-phase is transformed into brittle oxygen stabilized α-Zr(O); for example at dT/dt = 5 K/s, the critical temperature for cladding embrittlement is about 1600°C.

Figure 4 shows cross sections and microstructures of the reaction layers of specimens which were heated and cooled at 5 K/s to various maximum temperatures. At a maximum temperature of 1400°C the internal and external reaction layers formed in the cladding as described in Figures 1 and 2. The prior β-phase is still dominant, which means that the cladding is still ductile. At a maximum temperature of 1600°C, the β-phase has disappeared and the cladding is embrittled. At 1800°C, the metallic part between the UO_2 and ZrO_2 looks like a solidified (U, Zr, O) melt. The ceramic phase whithin the metallic melt consists of an oxidic solid solution $(U, Zr)O_2$ which forms due to chemical interaction between the molten Zircaloy cladding and UO_2 or ZrO_2.

A comparison of the growth rate equations of the whole reaction zones for the UO_2/Zry, O_2/Zry, and H_2O/Zry reactions is shown in Figure 5. Note that the total UO_2/Zry growth rate curve overlaps the steam/Zry region (results of six investigations /2,3/) above about 1100°C. This means, that the UO_2/Zry reaction occurs as rapidly as the steam/Zry reaction above about 1100°C. The total growth rate curve for the O_2/Zry gas mixture lies within the steam/Zry region. For this reason, the

gas mixture (Ar+ 25 vol.% O_2), which was used in the MONA experiments, can be used to simulate a steam environment. This was also shown in other tests /11/.

The modeling the combined internal and external cladding interactions resulted in the PECLOX (pellet cladding oxidation) numerical model. PECLOX solves the Fick and Stefan equations. It predicts the formation, growth, and disappearance of the various interaction layers and the corresponding oxygen profiles as a function of temperature and time up to complete Zry cladding oxidation /7,8/. In this respect, the PECLOX model has major advantages over other models /9, 10/, which attempt only to simulate the kinetics of the system in the first stages of the process, when all interface movements obey parabolic rate laws (infinte systems). Figure 6 shows a comparison between experimental results and calculations for an isothermal fuel/cladding interaction experiment under oxidizing conditions at 1100°C. The phase boundary movements are plotted versus the square root of time. The agreement between experiment and calculation is satisfactory /8/.

Figure 7 shows the calculated oxygen concentration profiles for the combined cladding interactions at 1100°C after 3000 and 10,000 seconds reaction time. Oxygen diffuses into the Zircaloy cladding from the inside and the outside forming various interaction layers. The metallic (U,Zr) alloy forming between the two oxygen stabilized α-$Zr(O)_{a,b}$ layers contains only a small amount of oxygen. The β-phase saturates with oxygen (3000 s) and then finally disappears. After long reaction times the cladding will be completely converted to ZrO_2 since the oxygen potential is higher on the outside (H_2O) than on the inside (UO_2). The (U,Zr) alloy then transforms into $(U,Zr)O_2$ oxide. Swelling due to a density change of the reaction products occurs at the ZrO_2/α-$Zr(O)_c$ interface.

2.2 UO_2 Dissolution by Molten Zircaloy

The meltdown behavior of Zry cladding depends decisively on the extent of the cladding oxidation and on the possible formation of a ZrO_2 oxide layer during the heating period. However, the

oxygen uptake by Zry depends not only of the oxygen potential of the environment but also on the chemical interaction with the UO_2 fuel, which is determined by the fuel/cladding contact conditions, i.e., the external overpressure. This is shown in Figure 8 /12/. Two specimens were tested under inert conditions to a maximum temperature of about 2000°C with a heating rate of 10 K/s and external pressures of 1 and 40 bar argon.

At 1 bar, very little oxygen was taken up by the cladding during heating because there was no good fuel/cladding contact. The onset of melting of the cladding therefore remained at about 1760°C. When the melting point was reached, the molten Zry ran down the specimen and, because the oxygen content was low, reacted with the UO_2 and dissolved a relatively large amount of fuel (upper left photograph in Figure 8). The different phases forming when molten Zry dissolves UO_2 are shown in the higher magnification photograph (upper right): (a) a metallic α-Zr(O) phase containing some U, (b) a metallic U-rich (U,Zr) alloy phase, and (c) a ceramic $(U,Zr)O_2$ phase.

At 40 bar, α-Zr(O) was formed during heating (and cooling) due to the UO_2/Zry chemical interaction. The cladding therefore melted at a higher temperature than Zry low in oxygen. Only a small amount of localized melting and cladding relocation occurred leaving the fuel stack relatively undisturbed (lower left photograph in Figure 8). The higher magnification photograph (lower right) shows the identical formation of reaction layers away from the cladding breach as observed in the isothermal and temperature transient tests below the melting point of Zry-4 (Figure 1).

Under oxidizing conditions an oxide layer forms on the outer cladding surface during heating before the melting point of Zry or α-Zr(O) has been reached. Therefore, the relocation of molten material will be prevented. The molten cladding then interacts with UO_2 and ZrO_2 and may later breach the ZrO_2 shell. Studying the fuel dissolution by molten Zry requires a system in which no melt relocation occurs. For this reason, the reaction kinetics of molten Zry cladding with solid UO_2 fuel has been investigated in the LAVA high temperature melt

facility with UO_2 crucibles containing molten Zry /13, 14, 15, 16/. In these tests, small samples consisting of a UO_2 crucible and an as-received (oxygen-poor) Zircaloy melt specimen are heated in a larger tungsten crucible. The tungsten crucible acts as a susceptor for the induction heating and provides rapid heating of the test samples up to 2400°C. The temperature of the UO_2 crucible and tungsten susceptor is measured by a pyrometer during the test.

Below 1650°C the heating and cooling rate is limited to 1 K/s to prevent cracking of the ceramic crucible. Above 1650°C, the programmed heating rate increases to 5 K/s. The isothermal reaction time varies from 1 minute to 2 hours and molten Zircaloy/UO_2 tests have been run at reaction temperatures of 1950, 2050, 2150, and 2250°c. The temperature of the test specimen slightly lags behind the programmed temperature during heating. The measured temperature histories were used to obtain an effective reaction time for each test /16/.

At the end of each reaction test, a metallographic examination is performed on the crucible specimen. Figure 9 shows three specimens annealed at 1950°C for various reaction times /13, 15, 16/. The Zry melt interacts with the UO_2 crucible forming a (U,Zr,O) melt at temperatures which, on cooling, depending on the oxygen content, decomposes into either two metallic phases [α-Zr(O) and a (U,Zr) alloy] or into two metallic phases plus a ceramic $(U,Zr)O_2$ phase. Figure 9 shows the microstructure of the solidified (U,Zr,O) melts. The phases observed are in agreement with the U-Zr-O ternary phase diagram /1, 12, 15, 16/. The ceramic phase portion has been used to quantify the extent of fuel dissolution by molten Zry as functions of temperature and time /12, 13, 16/.

The uranium and oxygen content of the molten (U,Zr,O) mixture has been correlated to the area fraction of the $(U,Zr)O_2$ phase seen in the cross sections. The correlation was obtained by preparing control samples of known chemical compositions, heating them to a temperature above the melting point of the Zircaloy/UO_2 mixture and then examing the resulting microstructure /12,13,16/. Using the correlation between the

uranium or oxygen content and the microstructure, the dissolution rate of the UO_2 crucible in (wt.% UO_2)2/s was determined for these tests (Figure 10). The interaction obeys a parabolic rate law. At 2250°C/5 min the solidified (U,Zr,O) melt consists of 80 wt.% of dissovled UO_2 /13, 16/.

The significance of these experiments is that UO_2 fuel can be "liquefied" by molten Zry cladding about 1000°C below the melting point of UO_2 ($\approx$ 2850°C). As a result, fission gas release will be enhanced because the original UO_2 crystal structure is completely destroyed.

3. Out-of-pile Single Rod and Bundle Experiments

Under severe fuel damage conditions, the interaction between Zry and UO_2 described above competes with the oxidation of the cladding by steam. Also the interaction of fuel rods with grid spacers, guide tubes and absorber rods have an important influence on the damage behavior of the fuel element. To investigate the integral behavior of these competing effects, out-of-pile single rod and bundle experiments were started. The objectives of the tests are summarized in six categories:

- Competition between pellet/cladding chemical interaction and cladding oxidation by steam;
- influence of the exothermal zircaloy/steam reaction on the temperature increase (uncontrolled temperature escalation);
- oxidation behavior of liquid zircaloy;
- fragmentation of the fuel rods and the refrozen melt by embrittlement due to oxidation;
- influence of the absorber, guide tube and spacer materials;
- reference experiments for the internationally performed in-pile-experiments on severe fuel damage.

The strong influence of the boundary conditions requires realistic simulation. For this purpose, the CORA-facility was built by the Central Engineering Department of KfK /27/. In this facility bundles of up to 7x7 rods of 2 meter length can be heated to about 2000°C in steam. Various internal fuel rod and external system pressures as well as quenching of the hot bundle at the end of the test can be simulated.

In the meantime, part of the test program for which no pressure simulation and quenching was needed, has been performed in the NIELS-facility.

Two main points were of interest in the NIELS experiments:

- The influence of the uncontrolled temperature escalation due to the exothermal zircaloy/steam reaction on the rate of temperature rise and maximum temperature and its consequences with respect to fuel element damage behavior.

- The influence of the absorber material on fuel element damage behavior. AgInCd is mainly used in PWR and B_4C in BWR.

3.1 The NIELS Facility

Figure. 11 shows the NIELS facility. On the left, one can recognize the insulation of the double-walled vessel, which is heated by oil to 130°C. The four windows allow the observation of the bundle and the internal insulation arrangement and the measurements of the bundle surface temperature with two-color pyrometers. The cover can be lifted for access to the bundle arrangement before and after the tests.

The picture in the middle in Figure 11 is a cross section of the vessel. The 3x3 bundle, connected to power at the top and the bottom by water-cooled electrodes, is insulated by 10 cm of ZrO_2 fiber-ceramics. The outer metal sheath of this insulation can be recognized on the right side in Figure. 11.

The single fuel rod simulator is made of a central tungsten heater of 6 mm diameter, which is surrounded by annular UO_2-

pellets and the normal PWR-Zircaloy-cladding of 10.75 mm outer diameter. The maximum length used was 40 cm. The simulators can be used as a single rod or in a bundle arrangement.

To simulate the influence of the neighbouring fuel rods with respect of the exothermal Zircaloy/steam reaction, and to ensure a proper steam flow, the bundle is surrounded by a Zircaloy shroud. Uniform steam distribution is guaranteed by the tube system at the lower end of the bundle.

3.2 Experiments on the Temperature Escalation Behavior

Earlier experiments have shown that the behavior of the fuel rod at high temperatures in steam is mainly influenced by the oxidation of the cladding. The degree of oxidation at a given temperature is fixed by the rate of temperature increase up to this temperature and the time at temperature. For Zircaloy-clad fuel rods the actual heating rate is influenced by the rate of oxidation. The reaction rate rises exponentially with temperature. A rise in temperature increases therefore the reaction energy and this raises the temperature. The temperature increase escalates uncontrolled. The temperature rises until the reaction rate decreases due to delayed oxygen diffusion and/or until the heat losses, which grow strongly with temperature, dominate.

The formation of the ZrO_2 oxide layer reduces further oxidation. The extent of the reaction layer growth decreases as the thickness of the oxide layer increases. Consequently, the experiments were performed so that the thickness of the oxide layer at the onset of temperature escalation was the main parameter.

Out of eleven experiments /17, 18, 19, 20, 24/ performed, results from two typical examples with high and slow initial heating rates are described. Figure. 12 indicates the surface temperature of the fuel rod in comparison to the electric power input as a function of time. Escalation starts at a higher temperature the lower the initial heating rate is.Once escalation has started, the temperature rises even for a

constant electric power input. After reaching a maximum temperature of about 2000°C the temperature drops at about 1°C/s, despite the constant electric power input.

Figure. 13 shows the posttest appearance of the fuel rod simulators each from 4 different directions. One recognizes the great difference in damage. In the test ESSI-7 only a thin oxide layer is formed, which is swept away by the molten Zircaloy cladding after reaching the melting point of Zircaloy. In contrast, for the slow heatup of ESSI-4/5 upon reaching the melting point of Zircaloy the cladding is completely oxidized, thus avoiding melting of the cladding and partial dissolution of the UO_2.

Bundle tests /21, 22, 23, 25, 26/ produced the same results for the temperature escalation and for fuel rod behavior. As in the single rod experiments, a temperature escalation to a maximum temperature of about 2200°C was observed. The post-test appearance of the ESBU-1 3x3 bundle is shown in Figure 14. The oxide layer formed during heating, was swept down by the molten Zircaloy along with the dissolved UO_2 into the lower part of the bundle where it solidified again. The bundle cross section was blocked with the exception of one cooling channel. The oxidation around this channel is evident from the black seam. The cross section also shows the central heaters, the dark annular UO_2 pellets, whose outer region is partially dissolved, and the refrozen metallic (U,Zr,O)-melt which is relatively homogeneous in its chemical composition.

Investigation of the solidified melt provides information on the degree of UO_2 dissolution by the molten Zry. The necessary basic information is derived from the experiments discussed in the first part of this paper. In the refrozen melt (Figure. 15) three phases are found: α-Zr(O), a metallic (U,Zr) alloy and a mixed $(U,Zr)O_2$ oxide. The existence of an oxidic $(U,Zr)O_2$ phase proves the dissolution of a remarkable amount of UO_2.

The temperature escalation tests can be summarized as follows: In all tests an uncontrolled temperature escalation due to the exothermal Zircaloy/steam reaction is observed. The maximum

cladding surface temperature measured was around 2200°C. The starting temperature of the escalation increases with decreasing initial heating rate. For fast heating rates, the runaway of the molten Zircaloy is the rate limiting process in the temperature escalation. A large amount of the UO_2 pellets is dissolved by liquid Zircaloy. For low heating rates, the formation of a thick protective ZrO_2 oxide layer limits the reaction energy. There is no remarkable chemical interaction between the oxidized cladding and UO_2.

3.3 AgInCd Absorber Experiments

A PWR fuel element consists of grid spacers, guide tubes and absorber rods, in addition to the UO_2/Zry fuel rods. The material preferred for the grid spacers is Inconel 718, but also Zircaloy is used. The guide tubes are made of Zircaloy or stainless steel. The absorber rods contain an (Ag80, In15, Cd5) alloy and are clad with stainless steel. The alloy melts at about 800°C.

In the absorber test /28/ of the NIELS facility a central absorber rod inside a guide tube was used in the center of the 3x3 bundle. The guide tube was aligned relative to the fuel rod simulators by two Inconel grid spacers at the 70 and 250 mm elevations.

The failure temperature of the absorber rods in dependence on the guide tube material is given in the table below:

AgInCd-Absorber Test Matrix

Test	Max. temp. in the bundle	Failure temp.	Guide tube material
ABS-4	1170°C	no failure	Zircaloy-4
ABS-3	1400°C	1200°C	"
ABS-2	1850°C	1200°C	"
ABS-1	2050°C	1200°C	"
ABS-6	1400°C	1350°C	stainless steel

The influence of absorber alloy melting at 800°C becomes apparent in the fuel element when the stainless steel of the absorber rod fails. The failure temperature of the absorber rod

is therefore important for the failure behavior of the fuel element. The failure temperature of the absorber rod depends on the guide tube material. Experiments were performed with maximum bundle temperatures between 1170 and 2050°C. With a Zry guide tube the absorber rod fails at about 1200°C. A stainless steel guide tube raises the failure temperature to about 1350°C.

The earlier failure of an absorber rod surrounded by a Zircaloy guide tube is caused mainly by the chemical interaction between the Zry guide tube and the Inconel grid spacer. Inconel reacts eutectically with Zircaloy forming liquid reaction products. This melt then chemically destroys the stainless steel cladding of the absorber rod. The liquid (Ag, In, Cd) alloy is released and interacts with the Zircaloy of the fuel rod cladding. The resulting absorber/Zircaloy melt starts to dissolve the UO_2 pellets. These processes can release fission products due to failure of the cladding and cause dissolution of the fuel and blockage of the bundle far below the melting point of the Zircaloy ($\approx$ 1760°C).

Figures. 16 and 17 show the post-test appearance of the ABS-3 and ABS-1 absorber bundles. In ABS-3 the experiment was terminated shortly after failure of the absorber rod at 1200°C. The melt runs down into the lower part of the bundle where it freezes. The interaction between the molten absorber material and Zircaloy in this case is mainly limited by the zircaloy guide tube.

In the ABS-1 test, with a maximum temperature of 2050°C, damage is much more extensive. The Zry cladding has molten, dissolving the outer region of the pellets. The melt has solidified in the lower part of the bundle. On cooling the embrittled cladding and the pellets fragmented and have collected on the refrozen melt together with fragments of the shroud (Figure. 17).

Figure. 18 shows the refrozen melt in the lower part of the bundle after the rubble (debris) has been removed. Two separate regions are clearly recognizable. Figure. 19 shows their cross sections. Analysis of these cross sections shows that the lower

lump, which fills all of the inside of the shroud, consists mainly of absorber material (35 wt%), but contains also spacer material (30%), Zry (15%), and uranium (20%). The upper lump contains mainly uranium, with 10-12% Zr and less than 10% absorber and grid spacer materials. The cross sections in the lower lump show that the cladding was dissolved in the molten absorber material at temperatures far below the melting temperature of Zircaloy.

A filter was installed in the exhaust line of the vessel and the aerosol condensate was investigated by spectral analysis. The main component of the aerosols was Cd. For the ABS-1 test with a maximum temperature of 2050°C also 3.5 wt% Ag was found in the condensate. In agreement with these results, the analysis of the refrozen absorber melt in the lower part of the bundle showed that most of the cadmium had evaporated.

3.4 B_4C Absorber Experiments

In BWRs boroncarbid (B_4C) is preferentially used as absorber material. Figures 20 and 21 show the typical absorber rod and its arrangement within the fuel bundles. Inside the cross shaped absorber rod the boroncarbid is contained in stainless steel tubes. The blade of the absorber rod consists of stainless steel too. The absorber rod is surrounded by Zry cooling-channel boxes of the neighbouring fuel elements.

To get first information about the behaviour of B_4C in stainless steel two tests with the arrangement shown in Figure 22 have been performed: B_4C powder in a double stainless steel tube - simulating the absorber cladding tube and the blade - is heated in the center of a zircaloy-clad 3x3 bundle to 1800°C and 1300°C in steam. The posttest appearance of the bundle heated to 1800°C is given in Figure 23. Cross sections of the absorber rod with a maximum temperature of 1300°C at its hottest elevation are shown in Figure 24.

Figure 24 proves that the melting of the stainless steel tube started at the inside of the double tube, though the temperature is higher on the outside due to the geometrical

arrangement of the bundle. B_4C interacts eutectically with the components of stainless steel (Fe, Cr, Ni) resulting in the formation of liquid reaction products already below 1200°C as was shown by single effects tests. Above 1200°C the interaction kinetics becomes very fast. Figure 25 shows the microstructure of the solidified B_4C/stainless steel eutectic after 15 min at 1230°C. More than 2 mm of the initially 3 mm thick stainles steel cladding wall thickness was consumed by the interactions with B_4C. The right picture in Fig. 25 shows a few B_4C particles surrounded by various reaction products.

The liquid reaction products interact with the zircaloy cladding of the neighbouring fuel rod simulators in melting down the sheath as can be seen in rods 7, 2 and 6 of figure 23. This interaction between the B_4C stainless steel eutectic and the zircaloy is of great importance for the behaviour of B_4C absorber rods in the neighbourhood of the zircaloy fuel element coolant-channel boxes, because they can fail far below there melting point.

The temperature increase of the experiment shows, that there is only a limited reaction of the boroncarbid with the steam. The liquid B_4C/Stainless steel interaction products is surrounding the boroncarbid particles and in this way reducing or even preventing the direct contact between boroncarbid and steam.

3.5 The CORA Facility

The CORA facility /27/ was built to simulate boundary conditions relevant to investigate the fuel element behavior under severe fuel damage conditions. Compared to NIELS, this facility offers the following additional possibilities:

- Quenching of the hot bundle at the end of the test to investigate the fragmentation of Zry cladding due to embrittlement by oxygen uptake.

- A maximum system pressure of 10 bar assures the necessary contact between cladding and fuel pellet to investigate the solid state reaction between Zry and UO_2.

- A maximum internal fuel rod pressure of 100 bar can be applied, which result in the cladding ballooning and burst, to investigate the influence of ruptured fuel rods on the damage behavior.

- Longer bundles with a total length of 2 m and a heated length of 1 m can be used.

- Larger bundles (max. 7x7 without the corner rods) can be employed.

A schematic cross section of the CORA facility is shown in Figure.26. The quench tube can be recognized below the bundle. It can be moved hydraulically around the bundle at the end of the test, in this way simulating a rising water level.

The high temperature shield can be lowered into the quench unit for easy access to the bundle setup before the test and for direct investigation of the damage without any handling or moving of the bundle after the test.

Figure. 27 shows a bundle of 25 rods before the test. The central part of the bundle is covered by a Zircaloy shroud. In the upper part the fuel rod simulators and one grid spacer can be recognized. On the right of the picture the connection tube to the steam superheater can be seen.

The results of scoping test B /29/ are given in Figure. 28 + 29. In this test Al_2O_3 pellets were used instead of the UO_2 pellets. The test showed a strong interaction between Al_2O_3 and Zry which resulted in an early meltdown of the fuel rod simulator far below the melting temperature of the Zircaloy and Al_2O_3 cladding. This result is important with respect to the behavior of the burnable poison rods in pressurized water reactors, which contain 1.4 wt% B_4C in sintered Al_2O_3 pellets inside the Zry cladding.

The test matrix for 15 planned tests in the CORA-facility is given in Figure. 30.

4. Conclusions

1. The UO_2/Zircaloy interaction is an oxygen diffusion controlled process and obeys a parabolic rate law.

2. The UO_2/solid Zircaloy reaction occurs at the same rate as the steam/Zircaloy reaction. Therefore, cladding oxidation (embrittlement) from both the outside and inside surfaces occurs four times faster than oxidation from either surface alone.

3. Up to about 9 vol.% of the UO_2 can interact chemically with the solid Zircaloy cladding (<1760°C). In a real fuel rod, complete release of volatile fission products in this region of the fuel must therefore be assumed to occur.

4. The numerical computer model PECLOX is able to calculate the movement of the reaction interfaces as well as the oxygen concentration profiles in the various interaction layers as a function of temperature and time up to the complete oxidation of the cladding.

5. The dissolution of UO_2 by molten Zircaloy (>1760°C) can be described by a parabolic rate law. The dissolution rate is found to have an Arrhenius dependence on temperature.

6. Solid UO_2 fuel can be "liquefied" by molten Zircaloy cladding about 1000°C below the melting point of UO_2. As a result, the release of volatile fission products will be drastically enhanced.

7. In all single rod and bundle experiments temperature escalation due to the exothermal Zircaloy/steam reaction was found. The starting temperature of the escalation increases with decreasing initial heating rate. In these tests a maximum cladding temperature of about 2200°C was measured.

8. For fast initial heating rates the runaway of the molten Zircaloy is the limiting process for the temperature

escalation. A large part of the UO_2 pellet is dissolved by liquid Zircaloy.

9. For low heating rates the formation of a thick protective oxide layer limits the exothermal reaction energy. There is no remarkable interaction between the oxidized cladding and UO_2 fuel.

10. The failure temperature of the (Ag, In, Cd) absorber rods is influenced by the guide tube material. The absorber rods fail at 1200°C with Zry guide tubes and at 1350°C with stainless steel guide tubes.

11. The molten absorber material dissolves the Zircaloy cladding of the fuel rods far below the melting point of Zry, which results in a low-temperature premature failure of the fuel rods. The mixture of molten materials dissolves the UO_2 pellets.

12. The molten absorber material and the chemically dissolved bundle components form large lumps on solidification in the lower part fo the bundle.

13. A layer of rubble was formed by the fragmented embrittled fuel rods on the solidified melt during cooling.

14. Cd is the main component in the aerosol formed from molten fuel element materials.

15. The failure temperature of the boroncarbid absorber rods is determined by eutectic reactions between B_4C and the stainless steel components at about 1200°C, which liquify the absorber rod cladding.

16. The molten B_4C/stainless steel reaction product is able to liquify the Zircaloy of the fuel simulator cladding already at about 1250°C.

17. The reaction between B_4C and steam is limited since the B_4C particles are surrounded liquid interaction products.

Acknowledgments

The design and the construction of the facilities and the performance of the experiments was only possible with the contribution of a great number of co-workers. We want to express our gratitude to K. Hain, T. Vollmer; F. Brüderle, W. Butzer, J. Hanauer, G. Harbauer, W. Leiling, E. Mackert, N. Paroth, F. Schloß, W. Stahl, R. Töpfer (IT) and J. Burbach, G. Gausmann, H. Metzger (IMF).

For the development of part of the instrumentation we thank H. Malauschek, W. Lange, K.P. Wallenfels.

The authours would particularly like to thank A. Fiege, PNS-PL for the many valuable discussions on the objectives of the program and the test matrix and Prof. Dr. W. Dienst and Dr. R.R. Hobbins (EG&G Idaho) for their thorough technical and editorial review of the manuscript.

Finally we thank Mrs. Ivanitsch for the careful typing of the manuscript.

The work was sponsored by "Projekt Nukleare Sicherheit" (PNS/KfK).

5. Literature

1. P. HOFMANN, C. POLITIS; The Kinetics of the Uranium Dioxide - Zircaloy Reactions at High Temperatures. Journal of Nuclear Materials, 87, (1979), p. 375-397

2. P. HOFMANN, D.K. KERWIN-PECK; UO_2/Zry Chemical Interactions and Reaction Kinetics from 1000 to 1700°C under Isothermal Conditions, KfK 3552 (1983)

3. P. HOFMANN, D.K. KERWIN-PECK; UO_2/Zry Chemical Interactions under Isothermal and Transient Temperature Conditions. J. of Nucl. Mat. 124 (1984) 80-105

4. P. NIKOLOPOULOS, P. HOFMANN, D.K. KERWIN-PECK; Determination of the Interfacial Energy and Work of Adhesion in the UO_2/Zircaloy Diffusion Couple, J. of Nucl. Mat. 124 (1984) 106-113

5. P. HOFMANN, D.K. KERWIN-PECK, P. NIKOLOPOULOS; Explanation of the UO_2 Zircaloy Reaction Layer Sequence in Terms of the Total Interfacial Energy of the Systems, J. of Nucl. Mat. 124 (1984) 114-119

6. P. HOFMANN, et.al.; Temperaturtransiente UO_2/Zircaloy-Reaktionsexperimente unter oxidierenden Bedingungen, PNS-Jahresbericht 1984, KfK 3550 (1985) p. 4200/76

7. P. HOFMANN, H.J. NEITZEL; External and internal Reaction of Zircaloy Tubing with Oxygen and UO_2 and its Modeling, Fifth Intern. Conf. on "Thermal Nuclear Reactor Safety", September 9-13, 1984, Karlsruhe, W. Germany, KfK 3880/2B, p. 1015

8. P. HOFMANN, H.J. NEITZEL; Experimental and Theoretical Results of Cladding Oxidation Under Severe Fuel Damage Conditons. 7th Intern. Conf. on "Zirconium in the Nuclear Industry", 24-27 June 1985, Strasbourg, France

9. D.R.OLANDER; The UO_2/Zry-Chemical Interactions, J. of Nucl. Mat. 115 (1983) 271-285

10. A. DENIS, E.A. GARCIA; A Model to Describe the Interaction between UO_2 and Zry in the Temperature Range 1000 to 1700°C. J. of Nucl. Mat. 116, (1983) 44-54

11. H. UETSUKA, P. HOFMANN; Reaction Kinetics of Zircaloy-4 in a (25% O_2/75% Ar) Gas Mixture from 900 to 1500°C under Isothermal Condition, KfK 3917 (1985)

12. P. HOFMANN, D.W. KERWIN-PECK; Chemical Interactions of Solid and Liquid Zircaloy-4 with UO_2 under Transient Nonoxidizing Conditions, International Meeting on "LWR Severe Accident Evaluation", August 28-30, Cambridge, MA. USA

13. P. HOFMANN, et.al.; Chemische Auflösung von festem UO_2-Brennstoff durch geschmolzenes Zircaloy-Hüllmaterial, PNS Jahresbericht 1985, KfK 4000 (1986), p. 4200-56-59

14. P. HOFMANN, S. HAGEN; Untersuchugen zu schweren Kernschäden, insbesondere die chemischen Wechselwirkungen zwischen Brennstoff und Hüllmaterial, KfK 4170 (1986) 251-319

15. W. DIENST, P. HOFMANN, D.K. KERWIN-PECK; Chemical Interaction between UO_2 and Zircaloy-4 from 1000 to 2000°C, Nuclear Technology, Vol. 65 (1984) 109-124

16. P. HOFMANN, H. UETSUKA; UO_2 Dissolution by Molten Zircaloy Cladding, to be published as KfK report

17. S. HAGEN; Out-of-pile Experiments on the High Temperature Behaviour of Zry-4 Clad Fuel Rods. KfK 3567 (1983).

18. S. HAGEN, H. MALAUSCHEK, K.P. WALLENFELS. S.O. PECK; Temperature Escalation in PWR Fuel Rod Simulators due to the Zircaloy/Steam Reaction: Tests ESSI 1-3, Test Results Report, KfK 3507 (1983).

19. S. HAGEN, H. MALAUSCHEK, K.P. WALLENFELS, S.O. PECK; Temperature Escalation in PWR Fuel Rod Simulators due to the Zircaloy/Steam Reaction: Tests ESSI 4-11, Test Results Report, KfK 3557 (1985)

20. S. HAGEN, S.O. PECK; Temperature Escalation of Zircaloy-Clad Fuel Rods and Bundles under Severe Fuel Damage Conditions. KfK 3656 (1983).

21. S. HAGEN, S.O.PECK; Out-of-pile Bundle Temperature Escalation under Severe Fuel Damage Conditions. KfK 3568 (1983)

22. S. HAGEN, H. MALAUSCHEK, K.P. WALLENFELS, S.O. PECK; Temperature Escalation in PWR Fuel Rod Simualtors due to the Zircaloy/Steam Reaction: Bundle Test ESBU 1, Test Results Report, KfK 3508 (1983)

23. S. HAGEN, H. MALAUSCHEK, K.P. WALLENFELS, B.J. BUESCHER; Temperature Escalation in PWR Fuel Rod Simulators due to the Zircaloy/Steam Reaction: Bundle Test ESBU 2A, Test Results Report; KfK 3509 (1984)

24. S. HAGEN, et. al.; Post Test Investigation for Single Rod Tests ESSI 1-11, KfK 3768 (1987)

25. S. HAGEN, et.al.; Post Test Investigations for Bundle Test ESBU-1, KfK 3769 (1986)

26. S. HAGEN, et. al.; Post Test Investigations for Bundle Test ESBU 2A, KfK 3789 (1986)

27. S. HAGEN, et.al.; CORA-Program. KfK 3677 (1986)

28. S.HAGEN, Damage Behaviour of (AgInCd)Absorber in PWR Fuel Rod Simulator Bundles under Severe Fuel Damage Conditions, Test Results Report, KfK 4102 (1987)

29. S. HAGEN, P. HOFMANN; Behaviour of B_4C-Absorber Rods under SFD Conditions, KfK 4103 (1987)

30. S. HAGEN, et.al., CORA Scoping Test B, Test Results Report, KfK 4171 (1987)

6. List of Figures

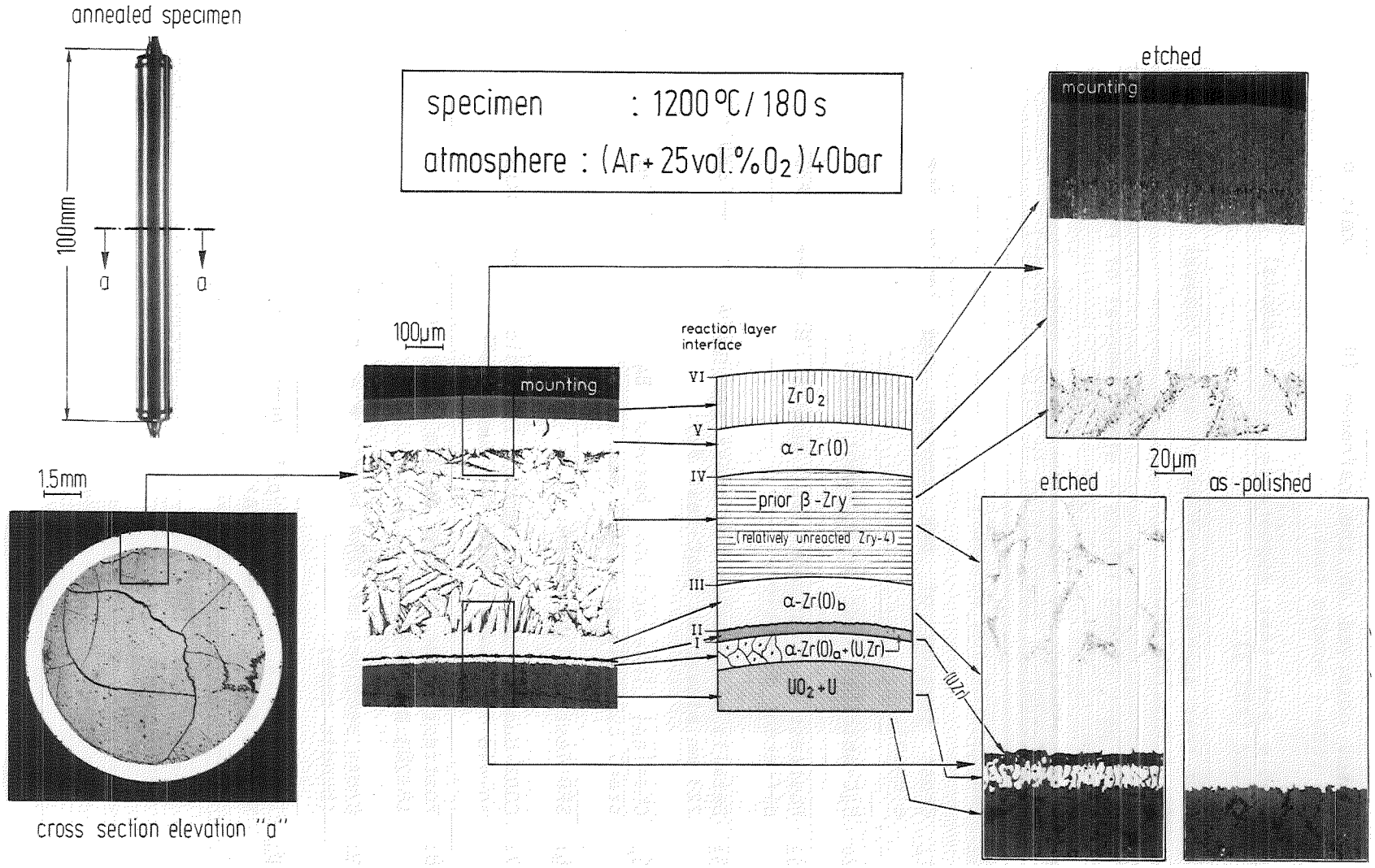

Fig. 1: Sequence of the external oxygen/Zircaloy and internal UO_2 /Zircaloy interaction layers.

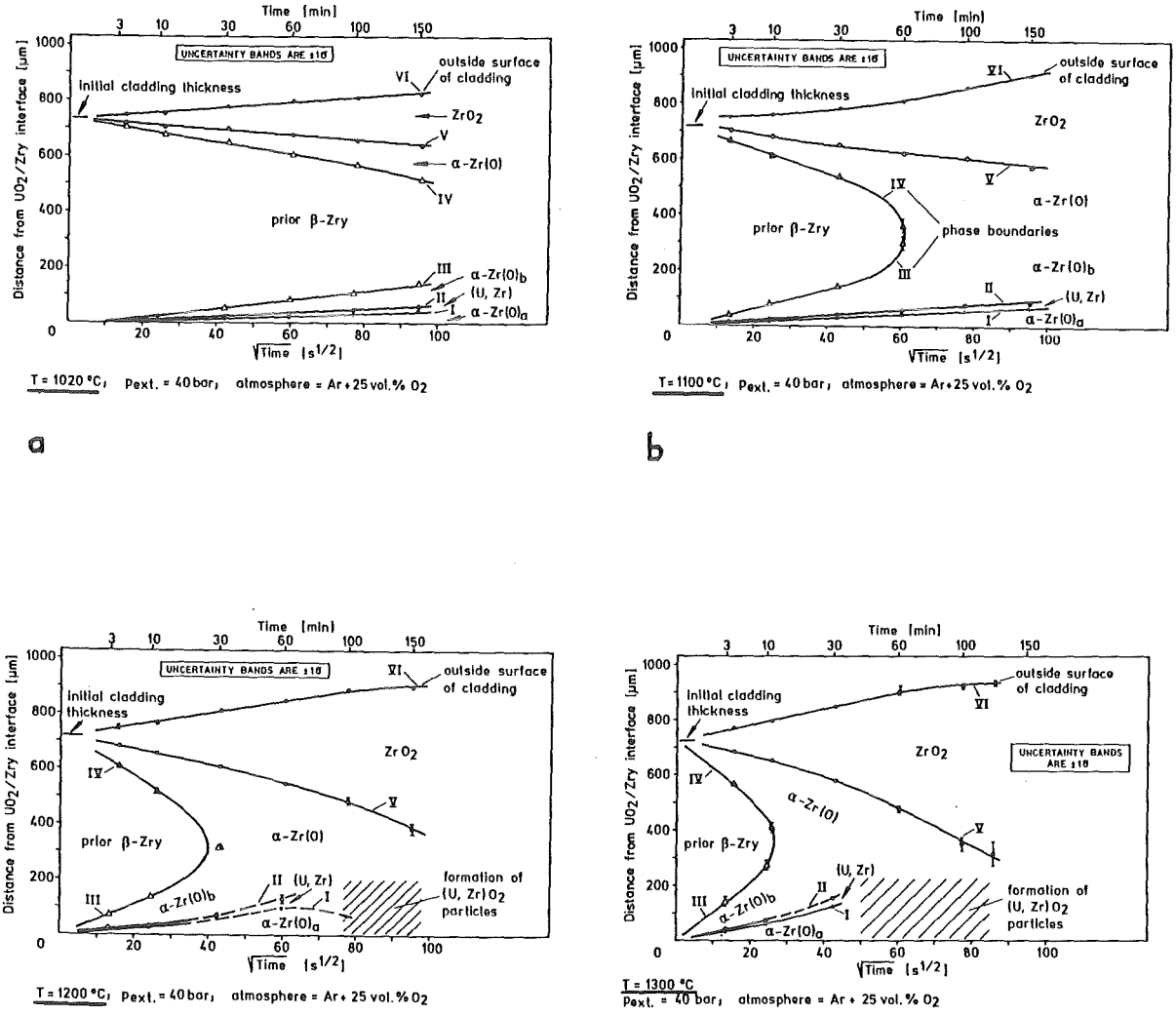

Fig. 2: Oxygen/Zirkaloy and UO_2/Zirkaloy reaction zone thicknesses as a function of $\sqrt{t}$ at a) 1020°C, b) 1100°C, c) 1200°C and d) 1300°C.

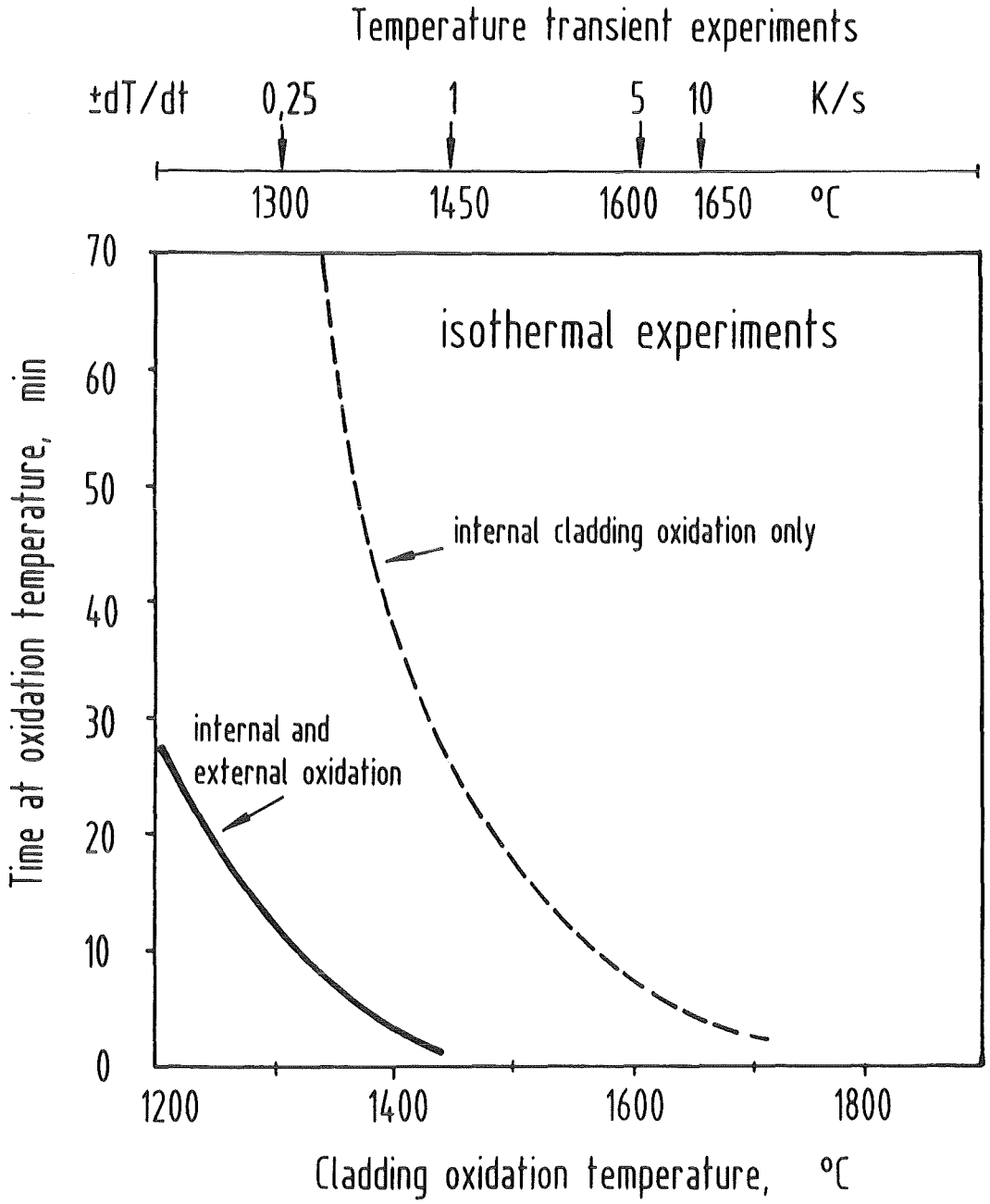

Fig. 3: Failure map for annealed LWR fuel rod segments. Zirkaloy embrittlement due to oxygen uptake.

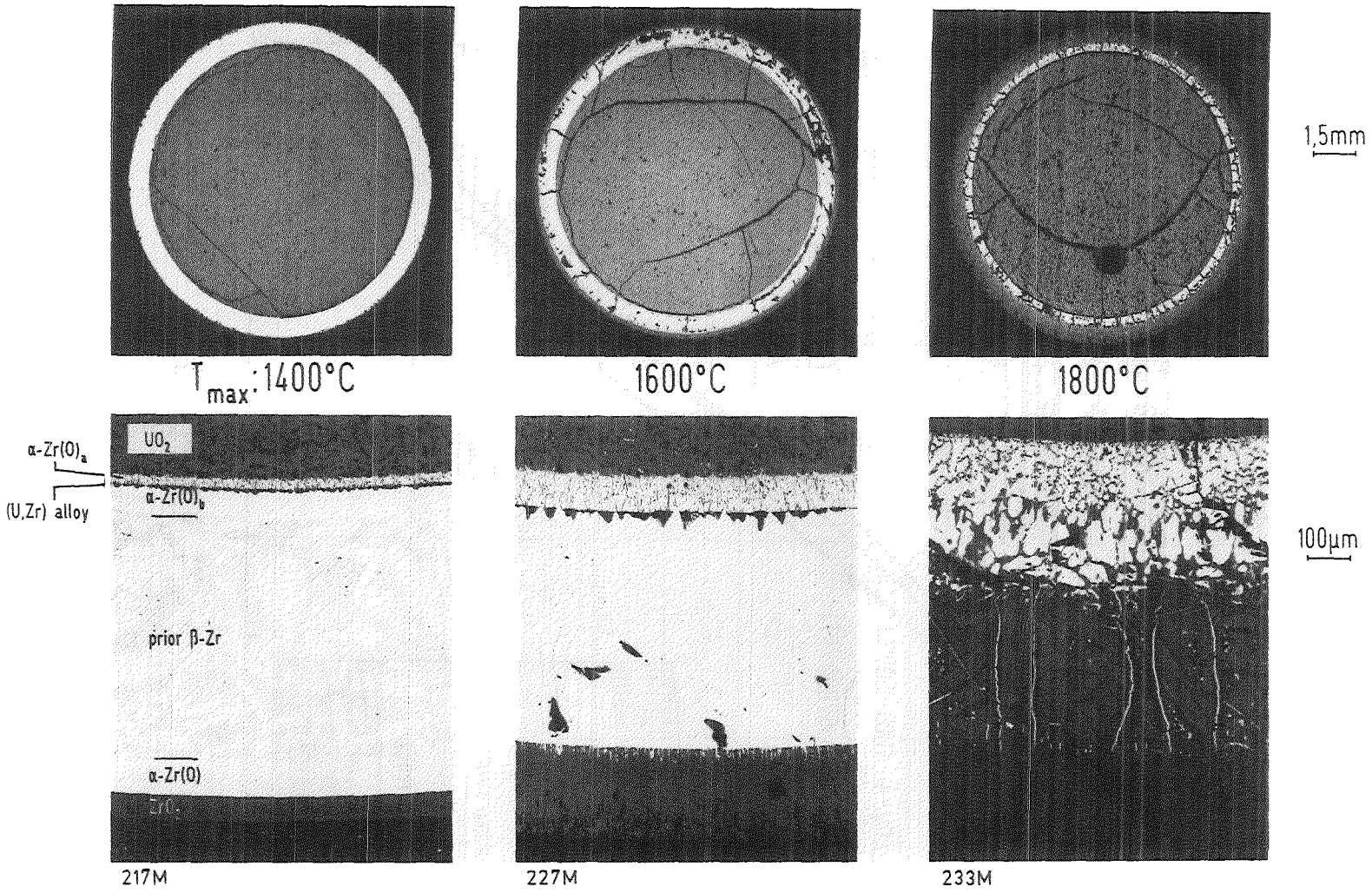

± dT/dt = 5K/s, atmosphere: (Ar + 25vol.%O_2), p_{ext} = 40bar

KfK

Fig. 4: Microstructure of transient heated fuel rod segments for various maximum temperatures at a heatup and cooldown rate of 5 K/s.

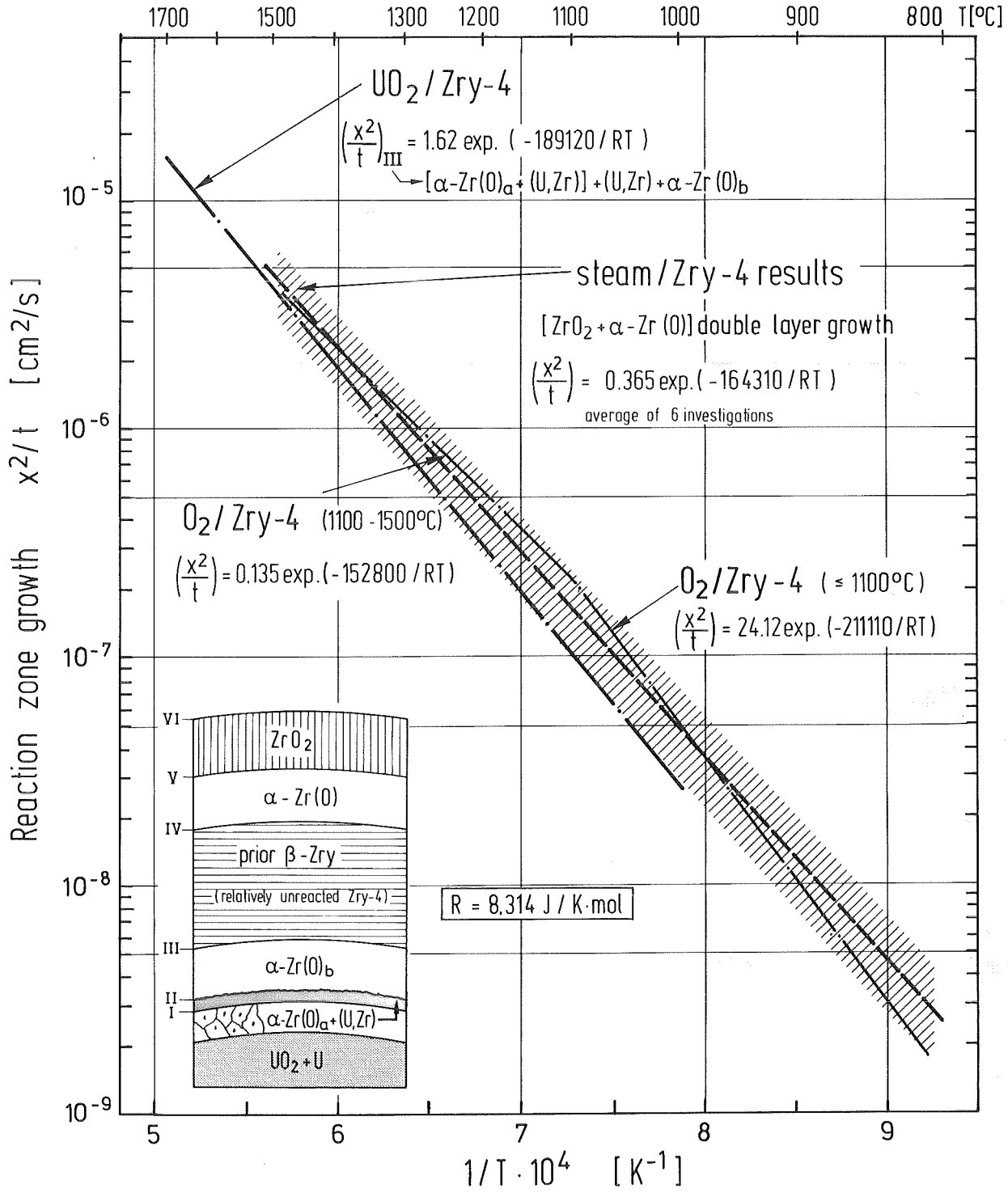

Fig. 5: Comparison of the growth rate for the UO_2/Zry, O_2/Zry and steam/Zry reactions

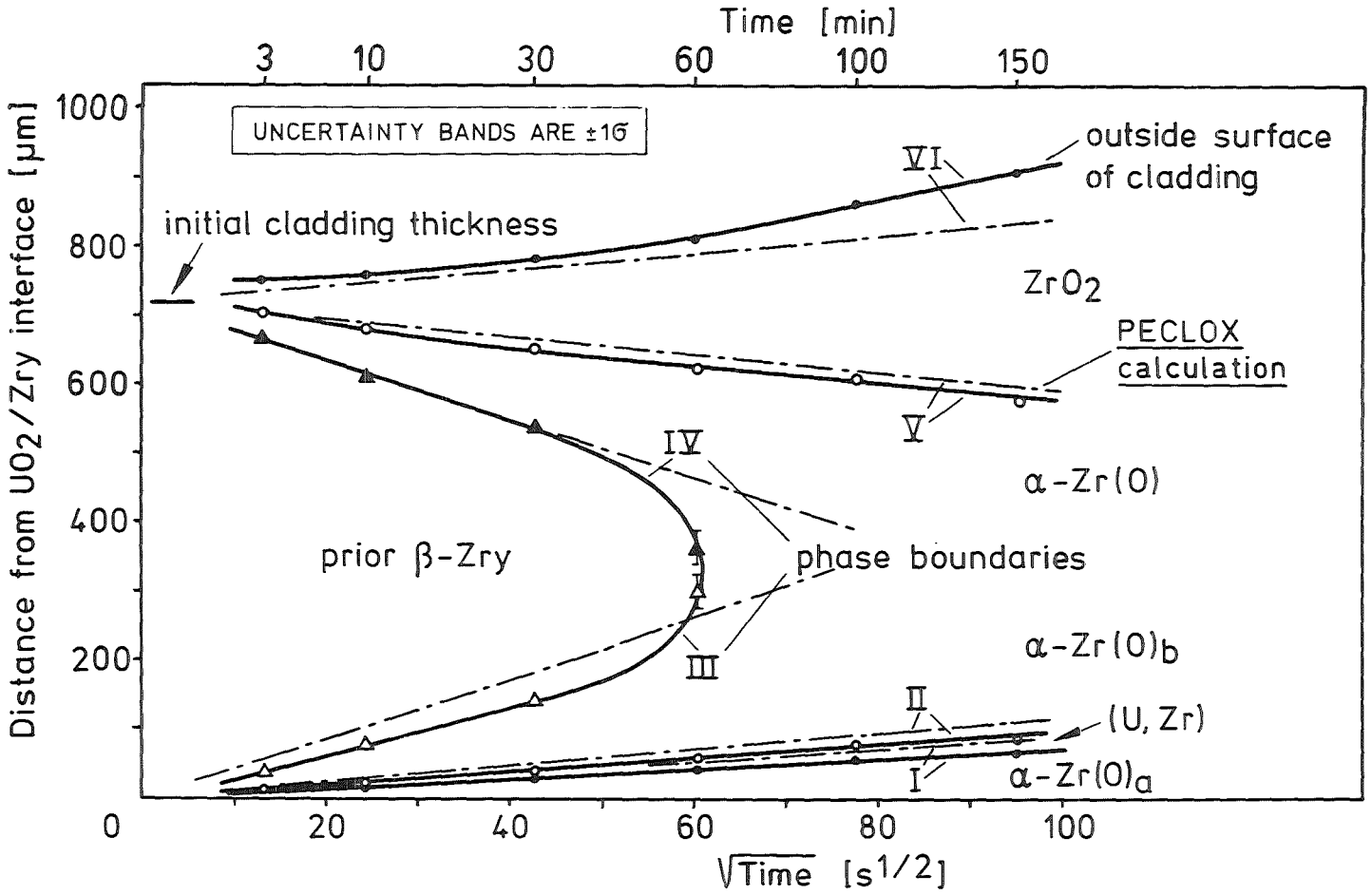

T = 1100 °C ; $p_{ext.}$ = 40 bar ; atmosphere = Ar+25 vol.% O_2

Fig. 6: UO_2/Zircaloy and oxygen/Zircaloy reaction zone thickness versus $\sqrt{t}$ at 1100°C. Comparison between experiment and PECLOX calculation.

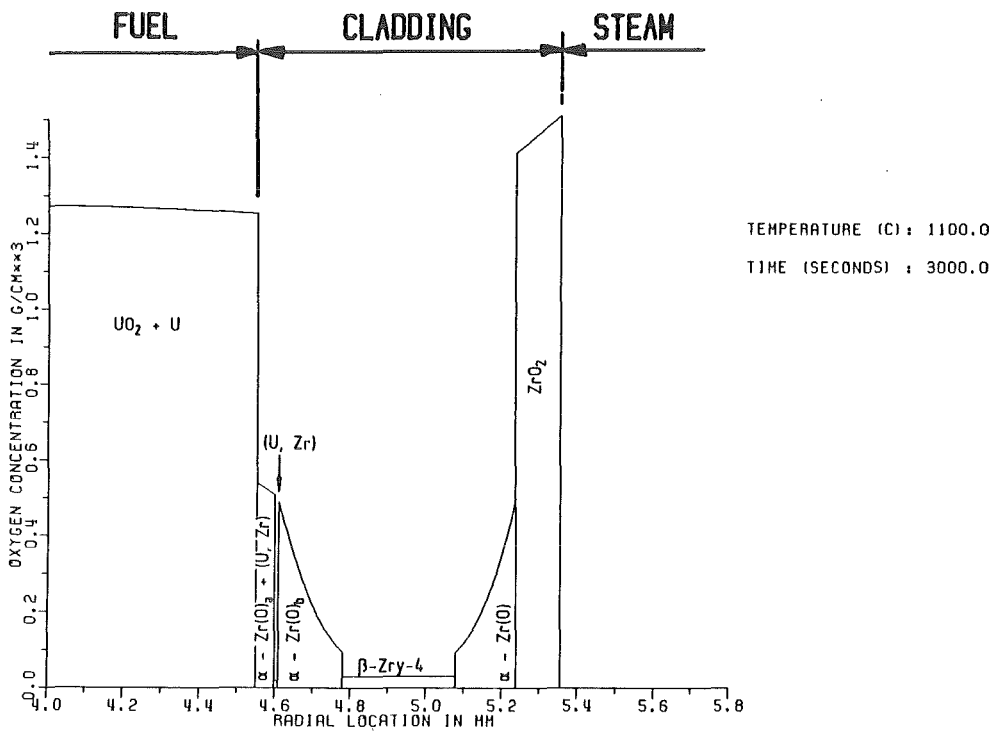

a) 3000s

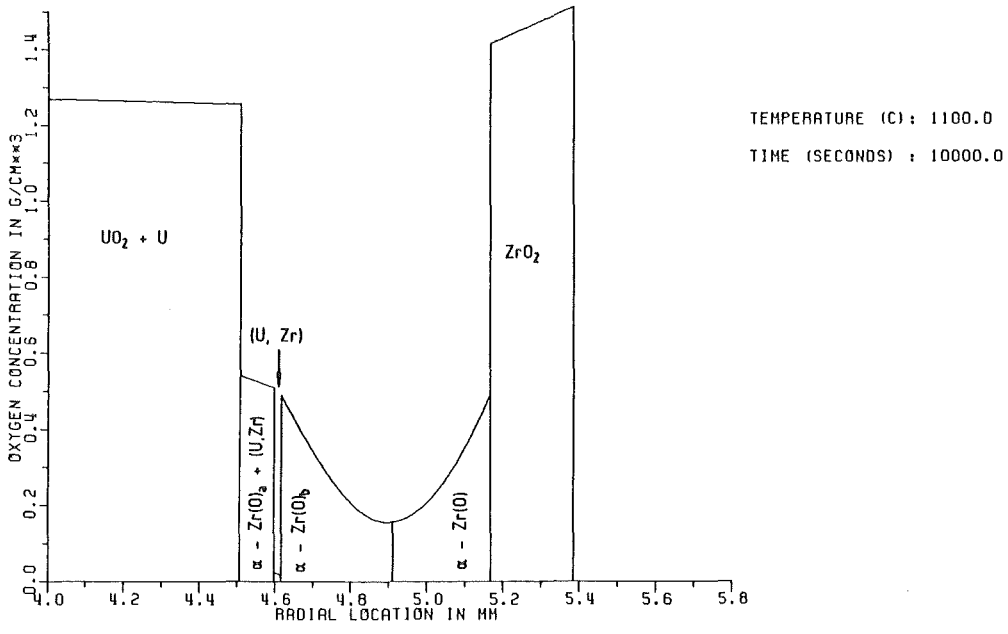

b) 10000s

Fig. 7:
UO_2/Zircaloy and oxygen/Zircaloy interactions at 1100°C. Oxygen concentration distribution in the various reaction zones for a) 3000s and b) 10000s reaction time.

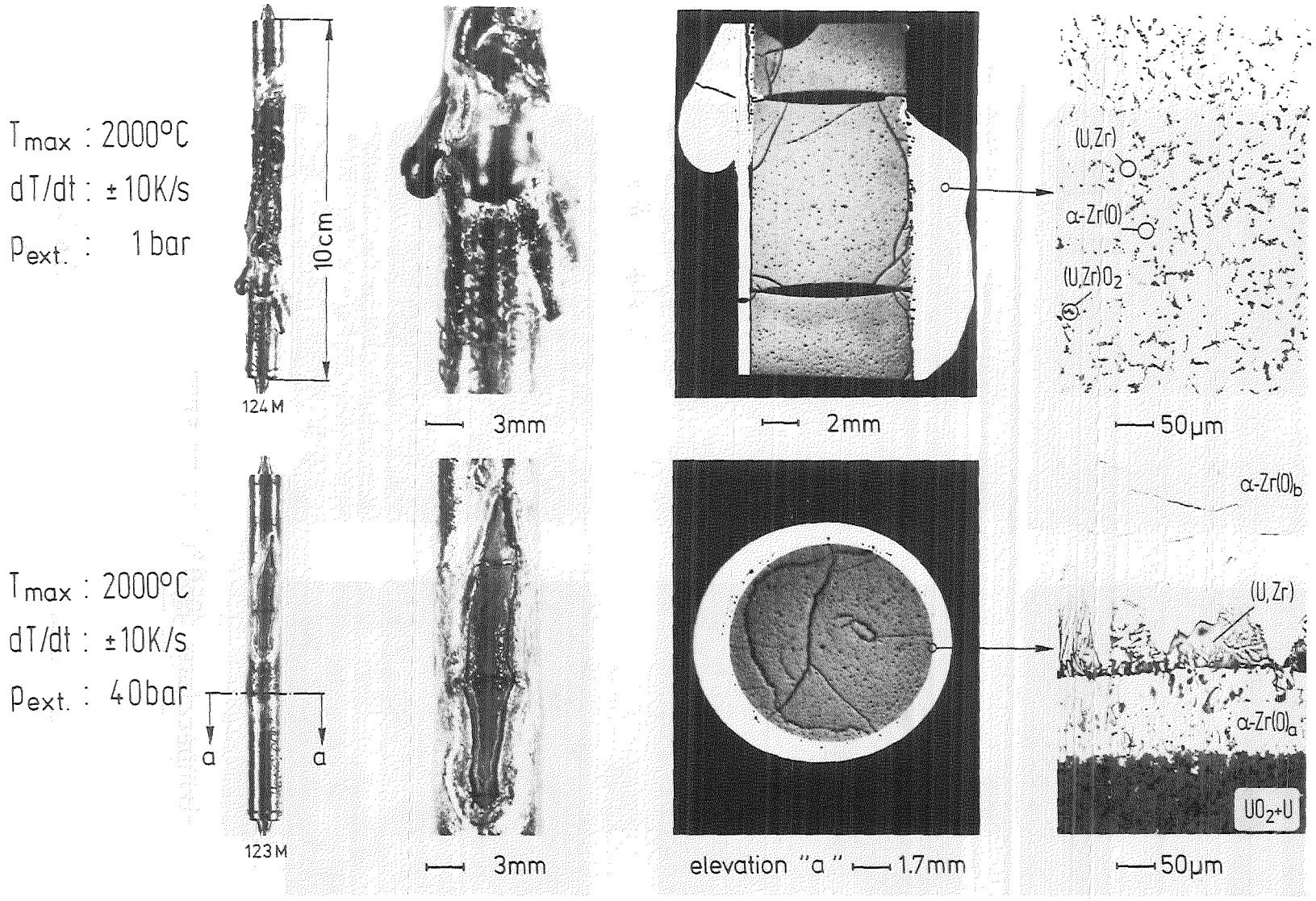

Fig. 8: Temperature transient UO_2/Zircaloy interaction experiments at 10 K/s up to about 2000°C as a function of external pressure (1 and 40 bar) under inertgas conditions.

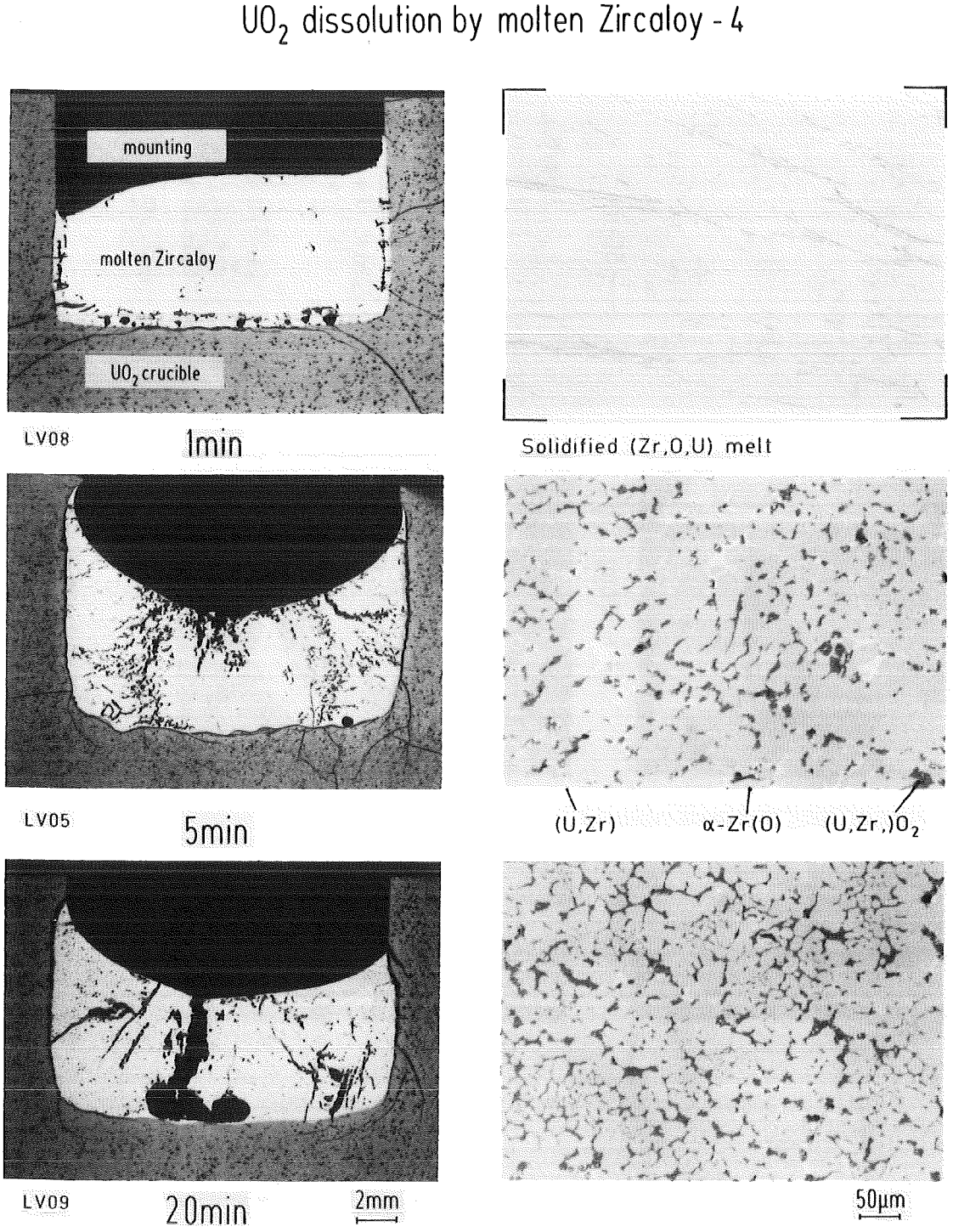

Fig. 9 : UO_2 dissolution by molten Zircaloy at 1950°C in Ar. Microstructure of solidified (Zr, U, O) melts as function of interaction time.

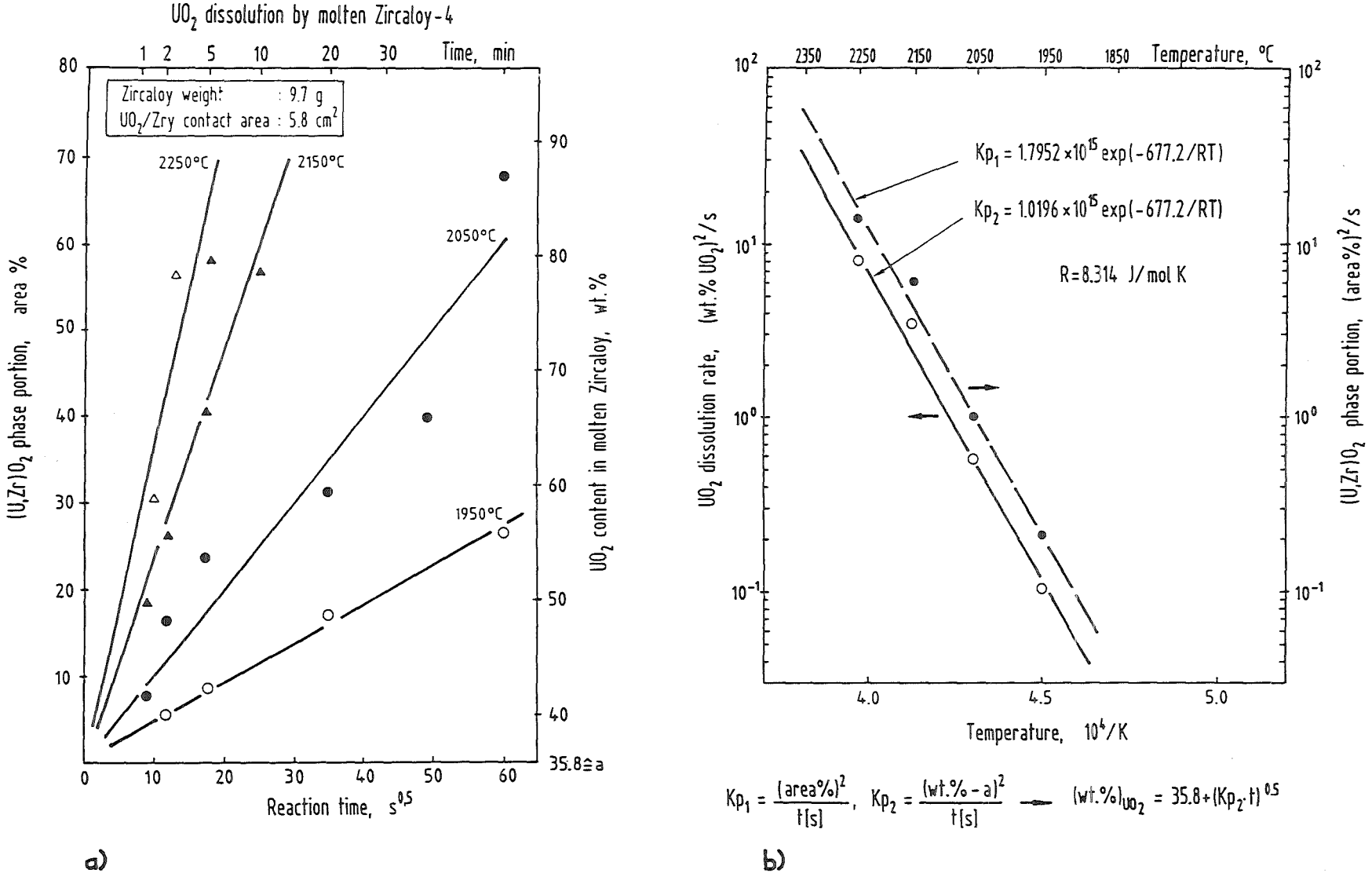

Fig. 10: UO_2 dissolution by molten Zircaloy. a) $(U,Zr)O_2$ phase portion in solidified (Zr, U, O) melts versus $\sqrt{t}$ for various temperatures. b) UO_2 dissolution rate.

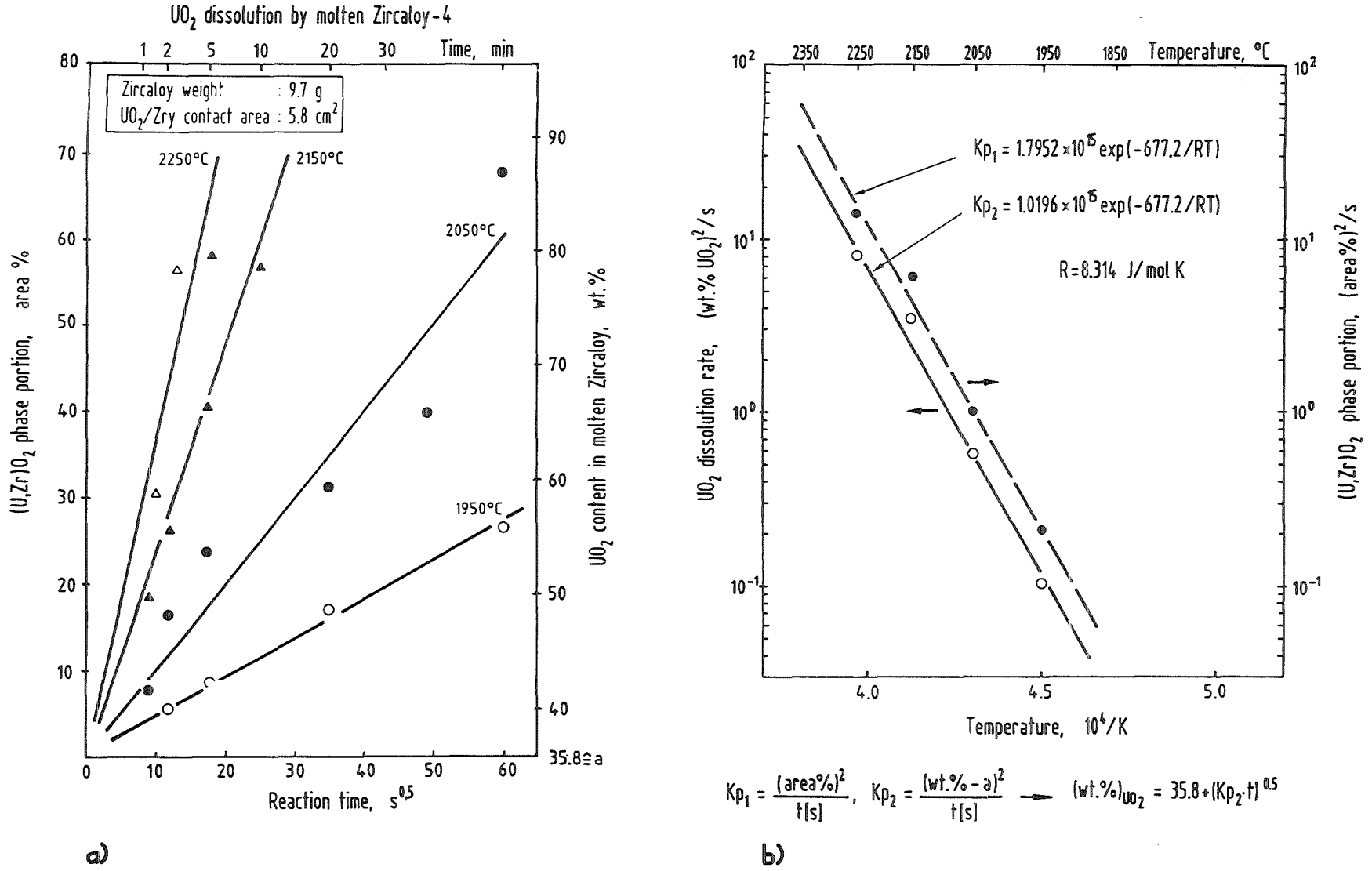

Fig. 10: UO_2 dissolution by molten Zircaloy. a) $(U,Zr)O_2$ phase portion in solidified (Zr, U, O) melts versus $\sqrt{t}$ for various temperatures. b) UO_2 dissolution rate.

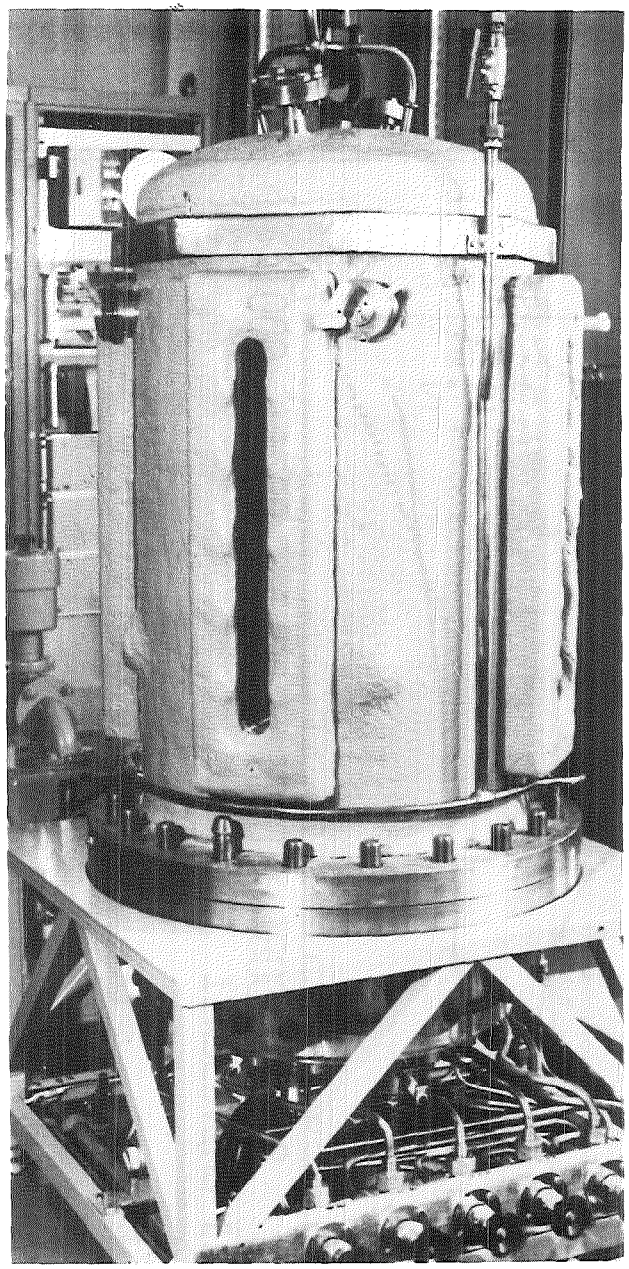

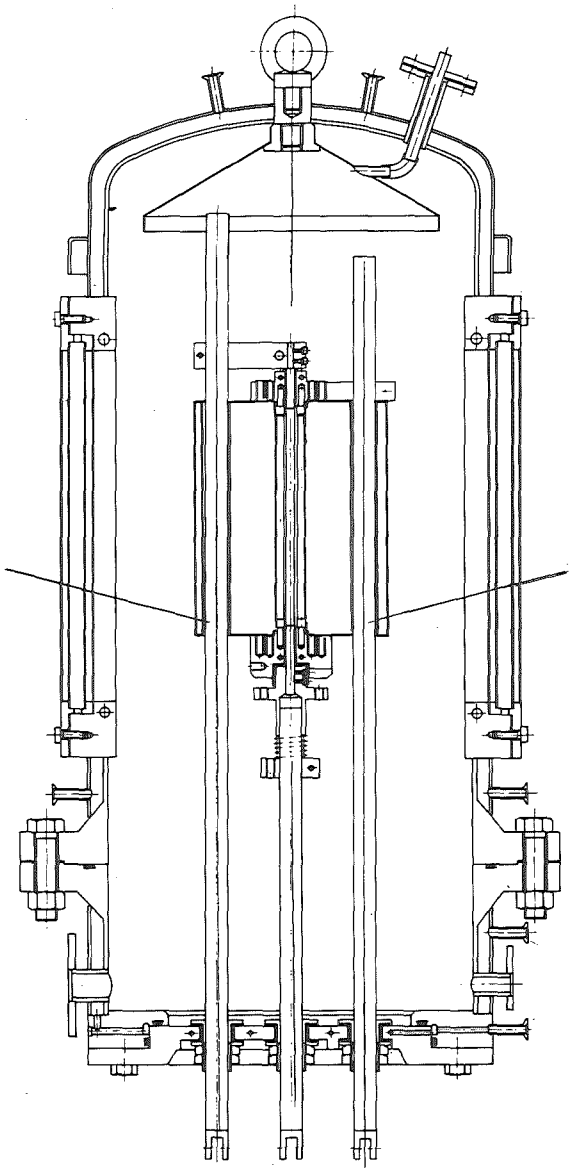

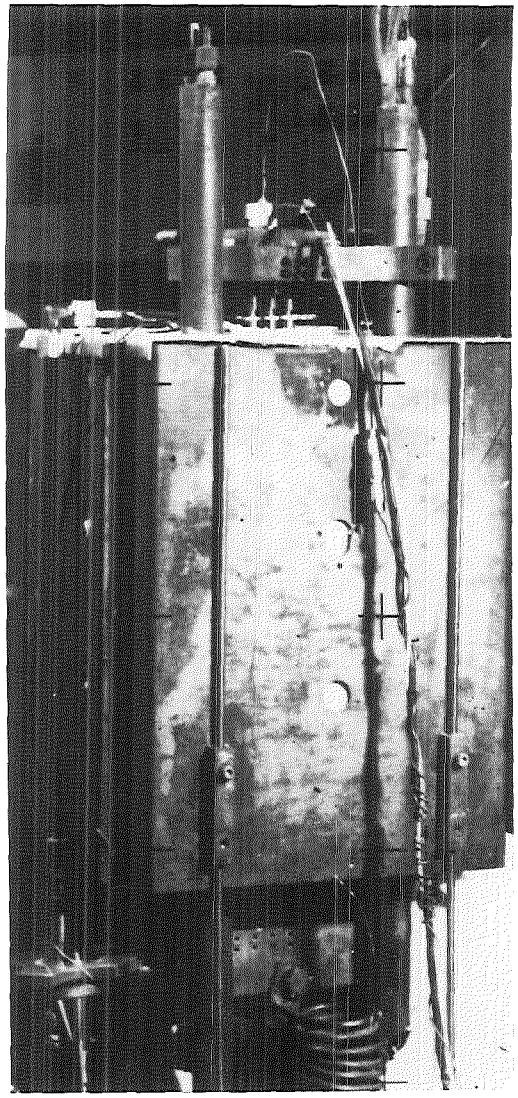

Fig. 11: Test Vessel, cross section and bundle insulation of the NIELS facility

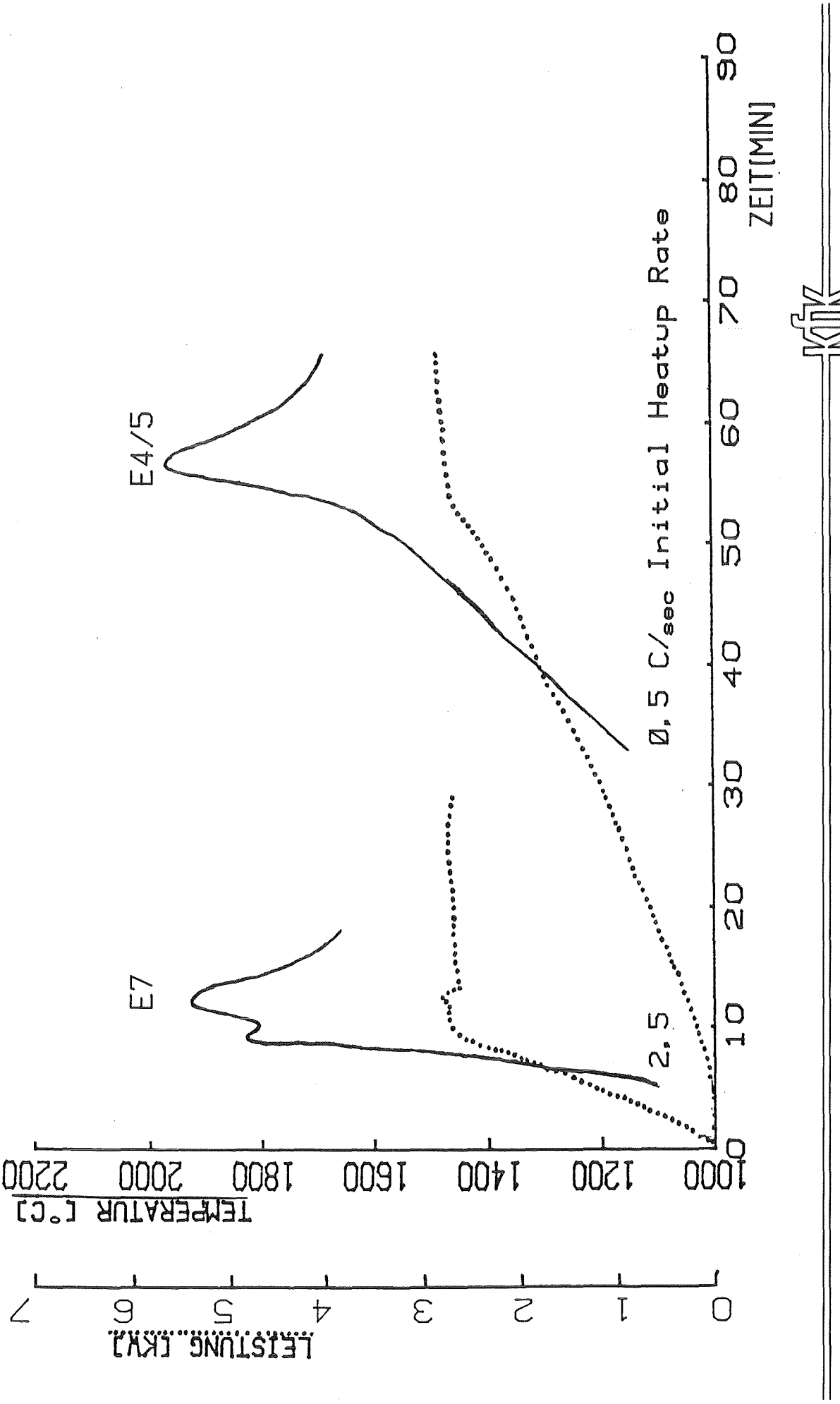

Fig.12 : Temperatures (-) on rod and electric power input (...) for test ESSI-7 and ESSI-4/5

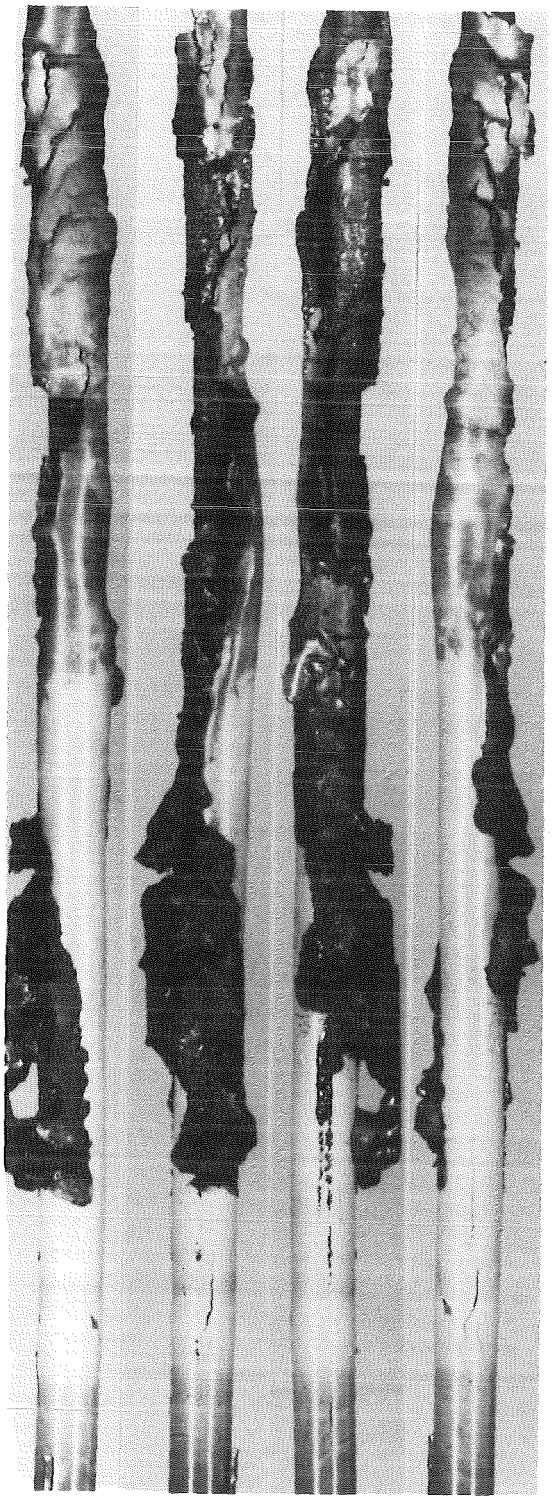

ESSI-7 (2,5°C/sec)

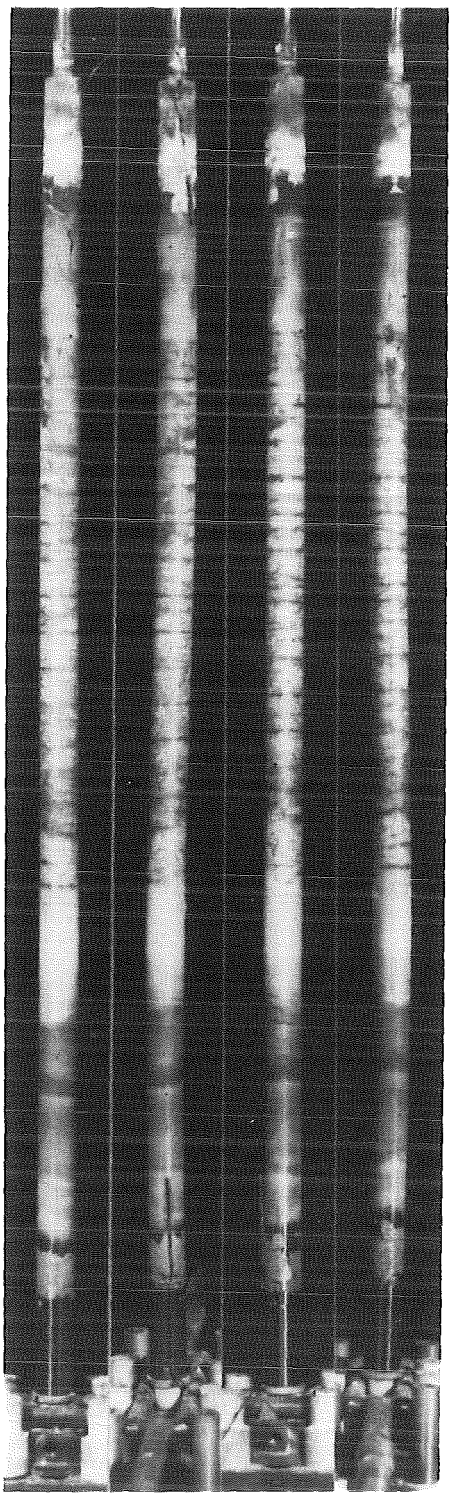

ESSI-4/5 (Ø,5°C/sec)

Fig. 13
FUEL ROD SIMULATOR POST TEST APPEARANCE FOR FAST (ESSI-7) AND SLOW (ESSI-4/5) INITIAL HEAT UP.

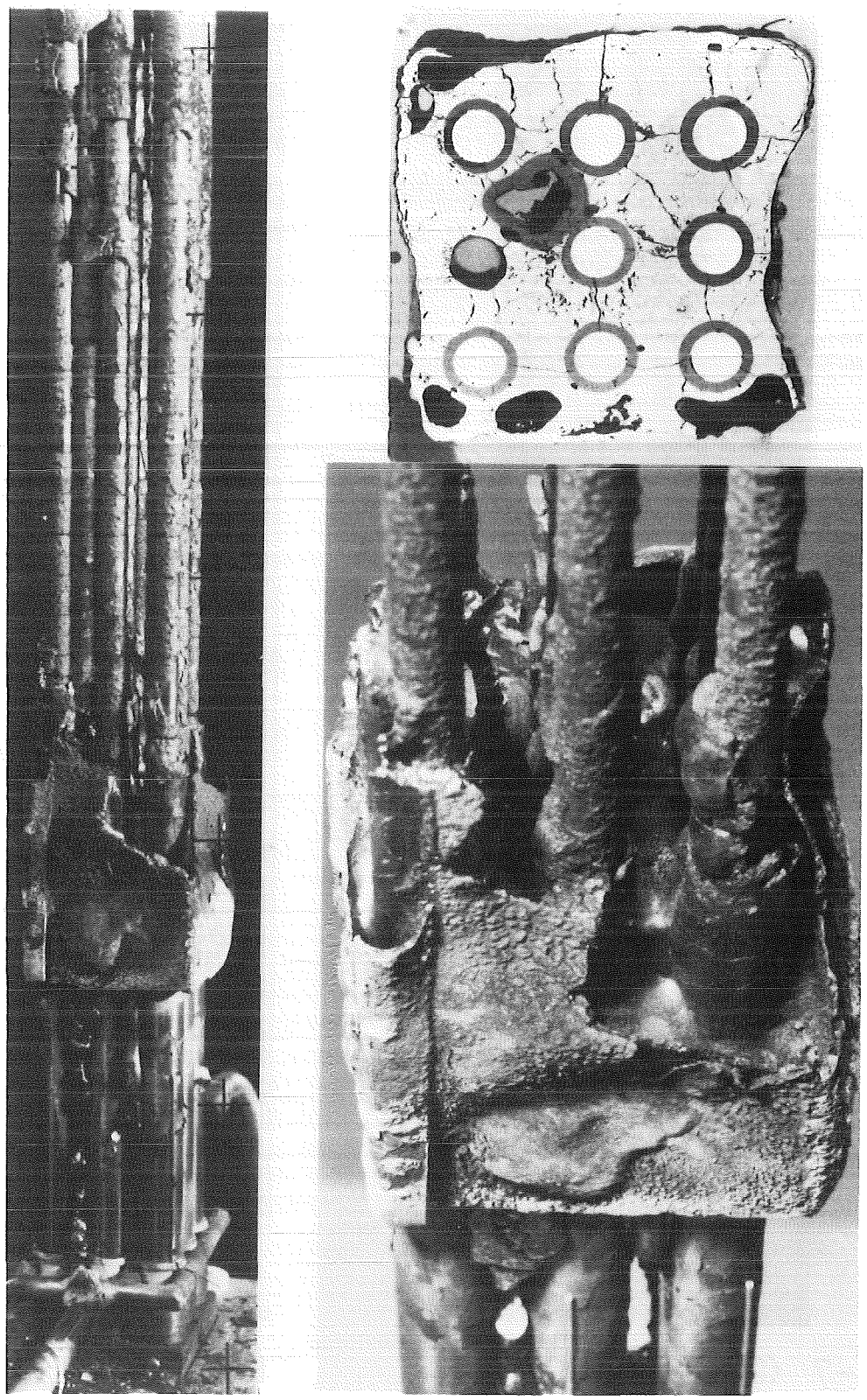

FIGURE 14 : POSTTEST APPEARANCE OF THE ESBU-1 BUNDLE AND A CROSS SECTION FROM THE RE-FROZEN MELT IN THE BLOCKED REGION (116 MM ABOVE THE BOTTOM OF THE BUNDLE)

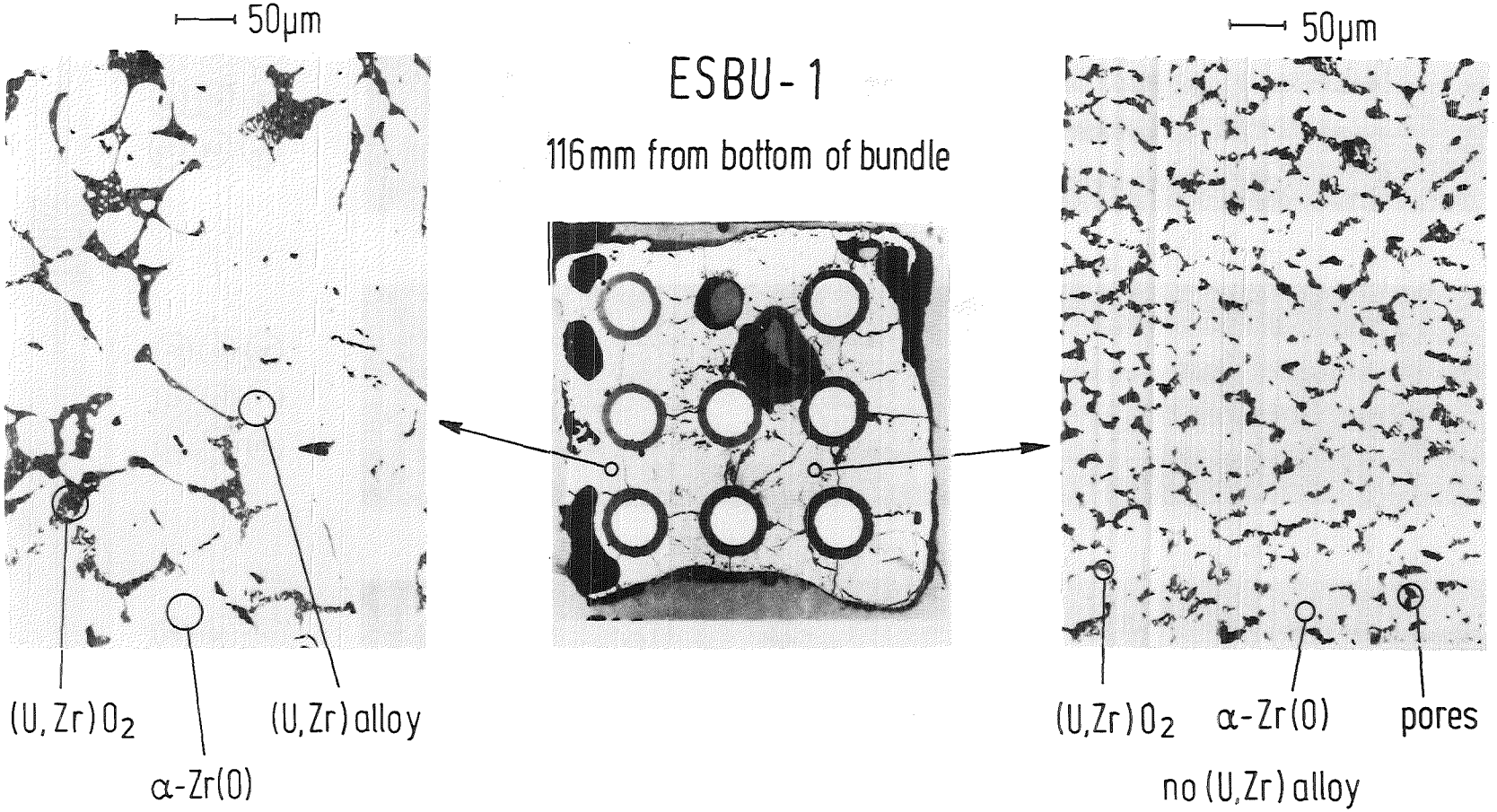

Fig. 15 : Phases found in the refrozen melt of bundle ESBU-1

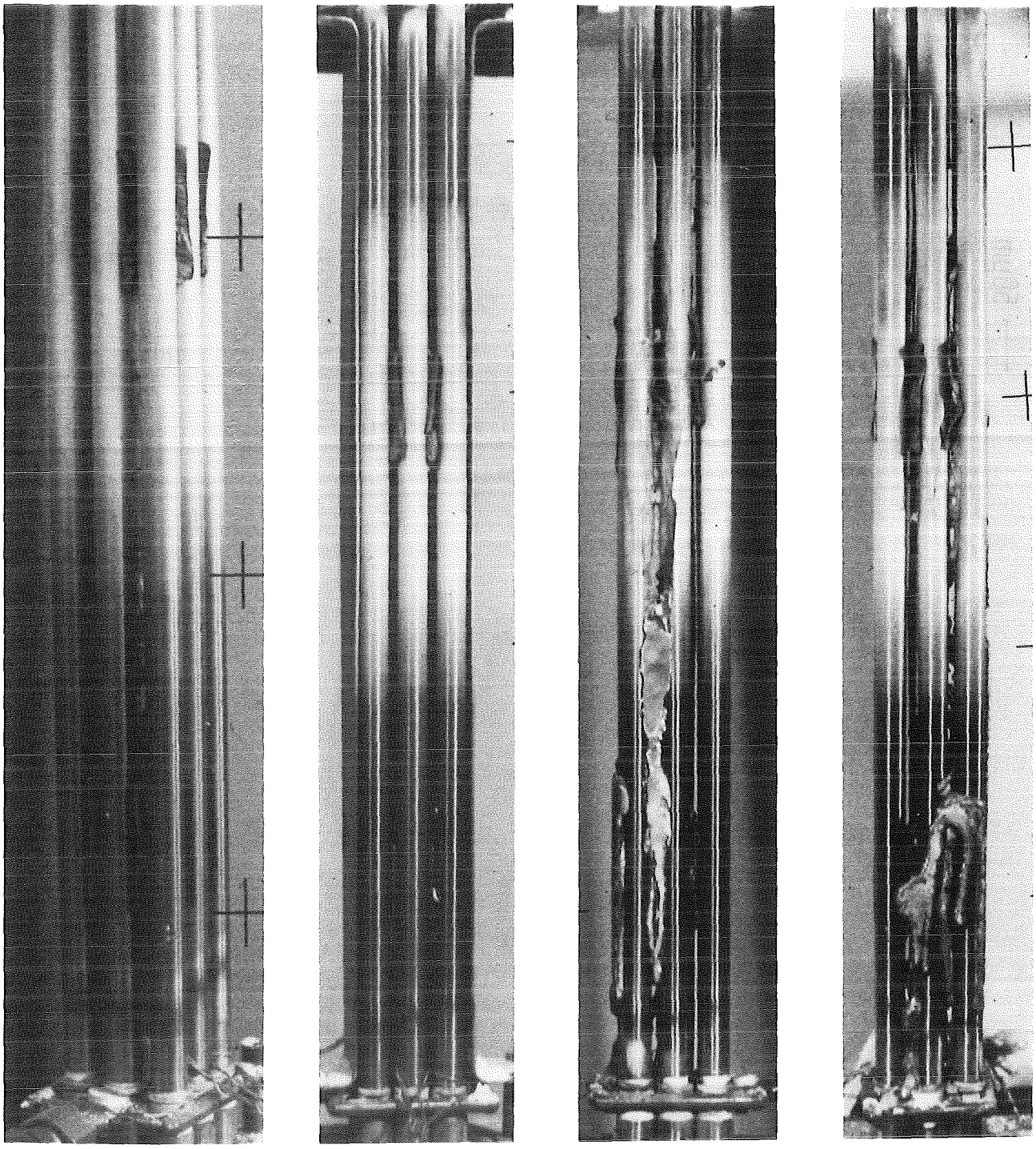

Fig. 16: Bundle posttest appearance after removing of shroud (ABS-3) (T_{max}=1400°C)

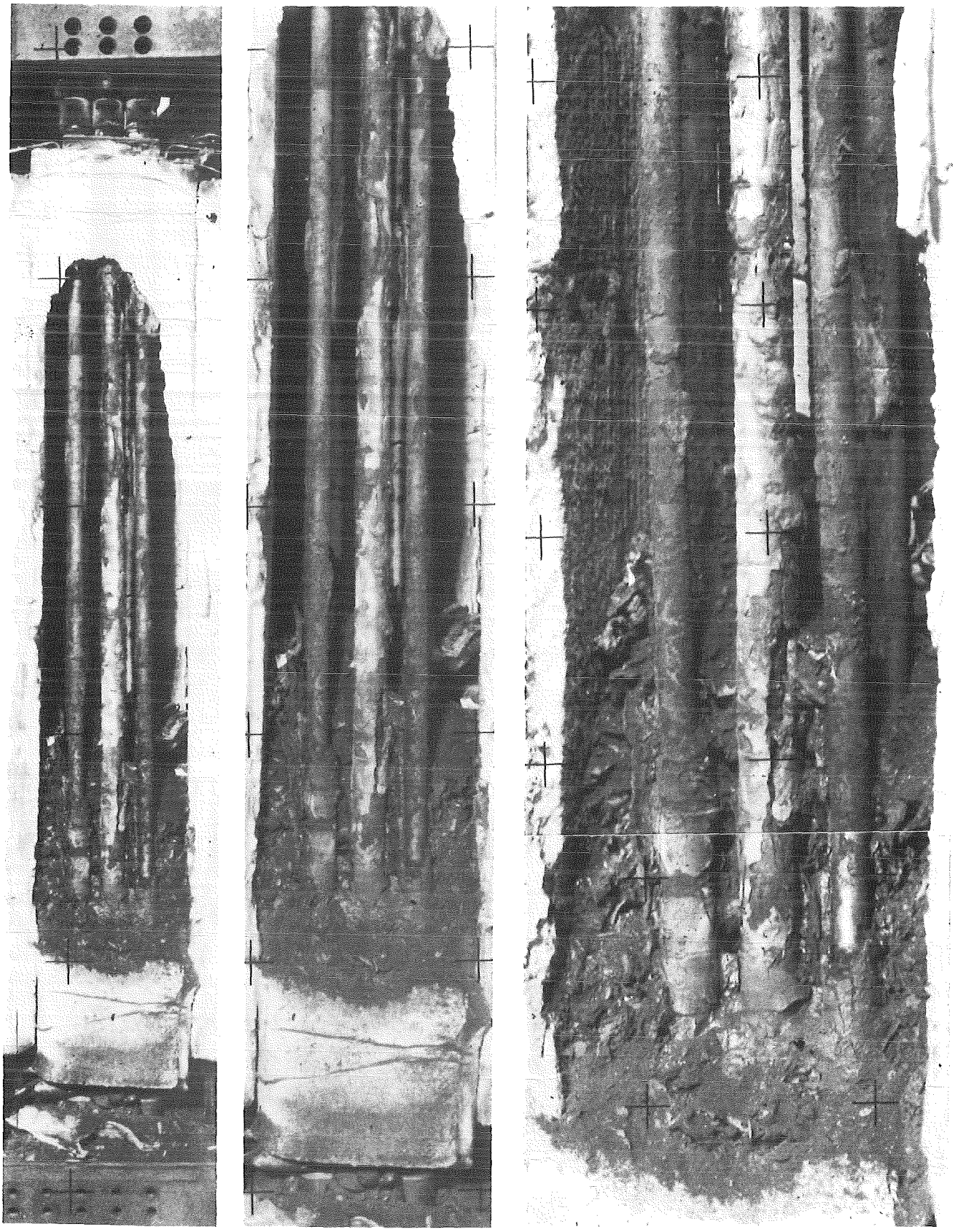

Fig. 17 Post test appearance of ABS-1 after removing of front isolation (T_{max}=2050°C)

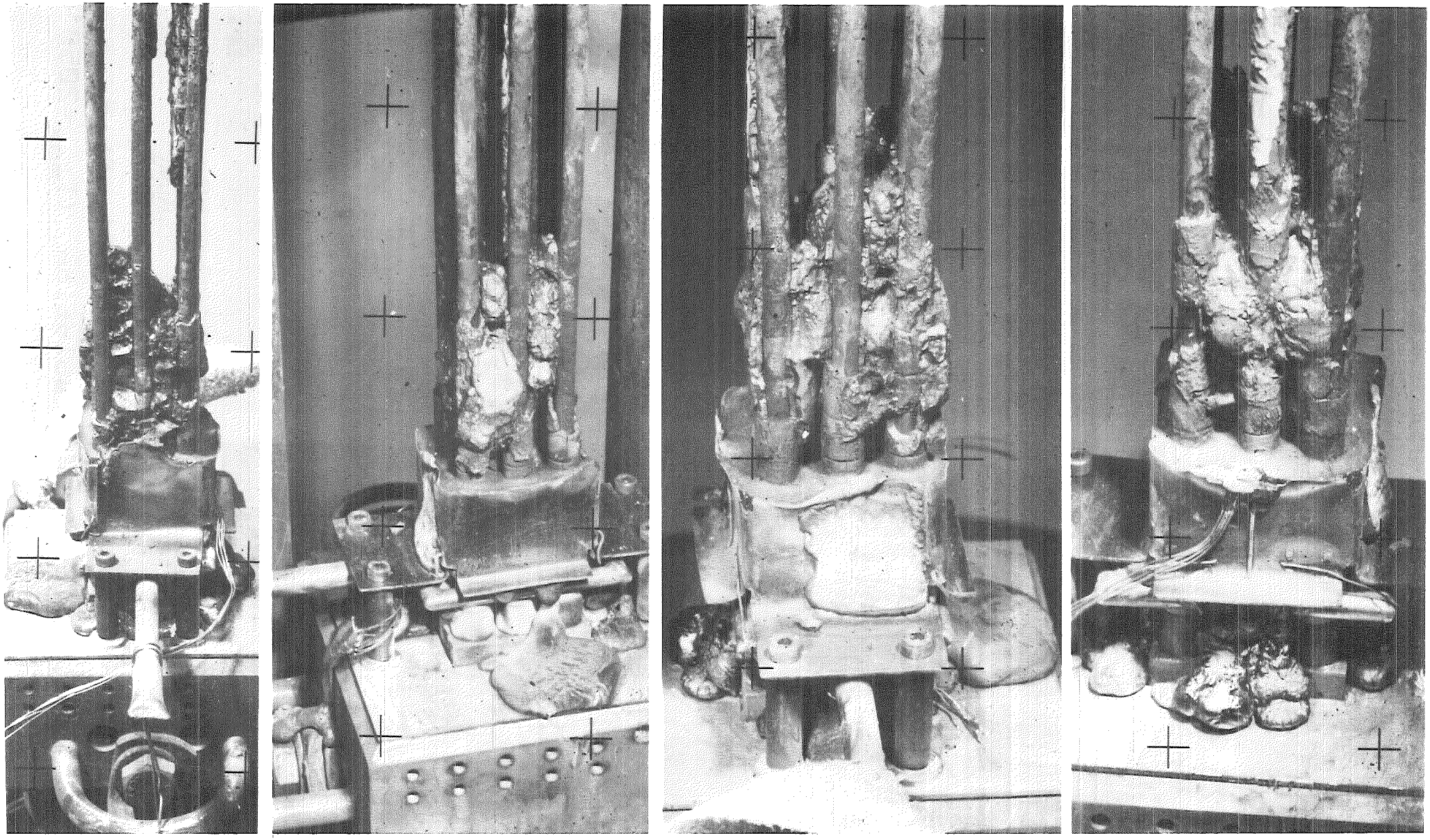

Fig. 18 *Lower part of bundle ABS-1 after removing of rubble*

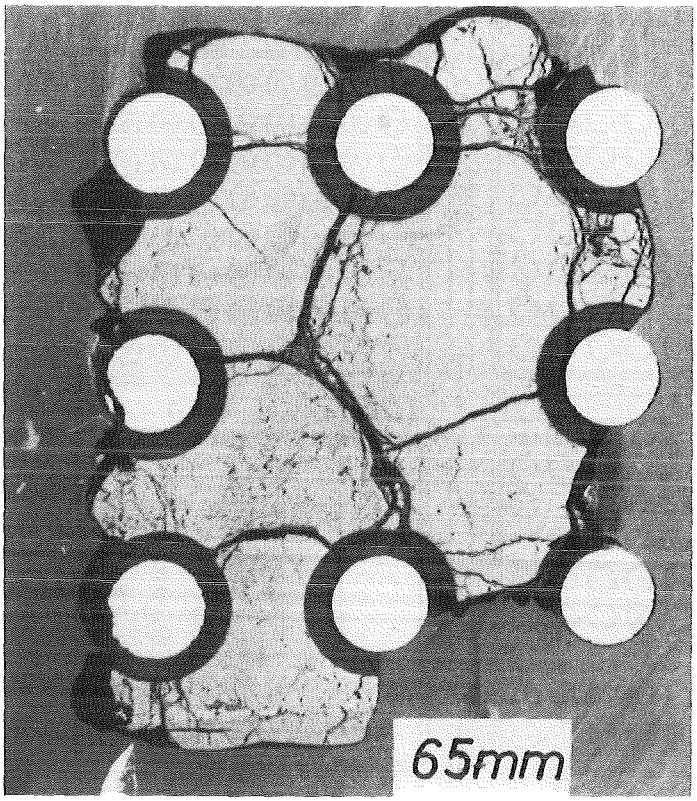

Main
Components:
U, Zr
(3% Fe)

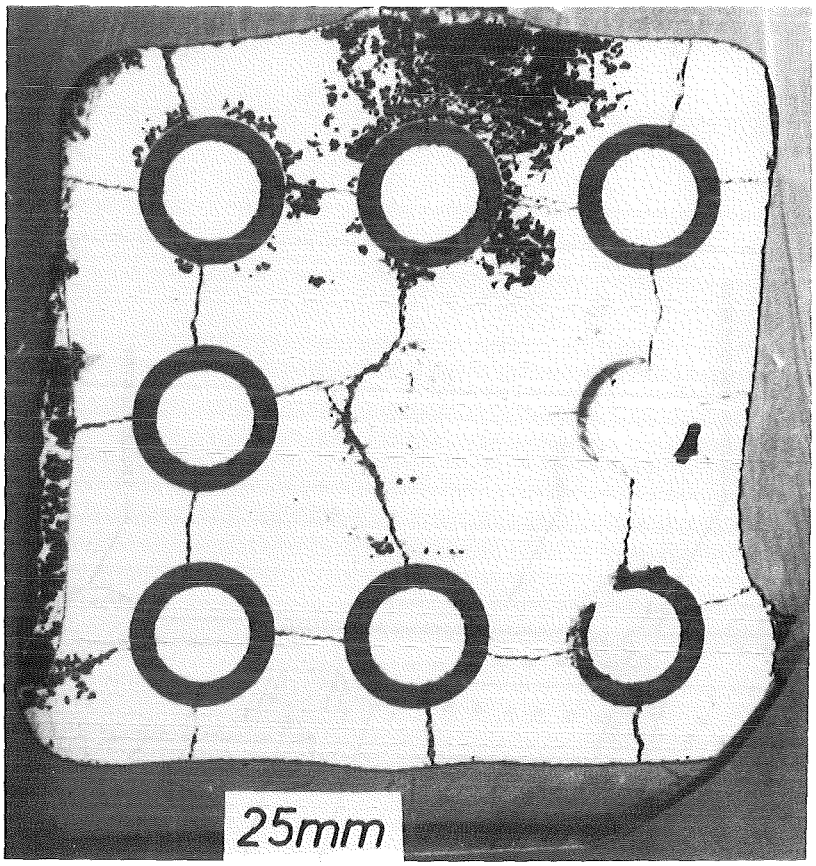

30% Ag
5% In
18% Fe
7% Ni
6% Cr
18% U
15% Zr

KfK

Fig. 19
Cross section of upper and lower lump in test ABS-1.
(chemical composition in weight percent)

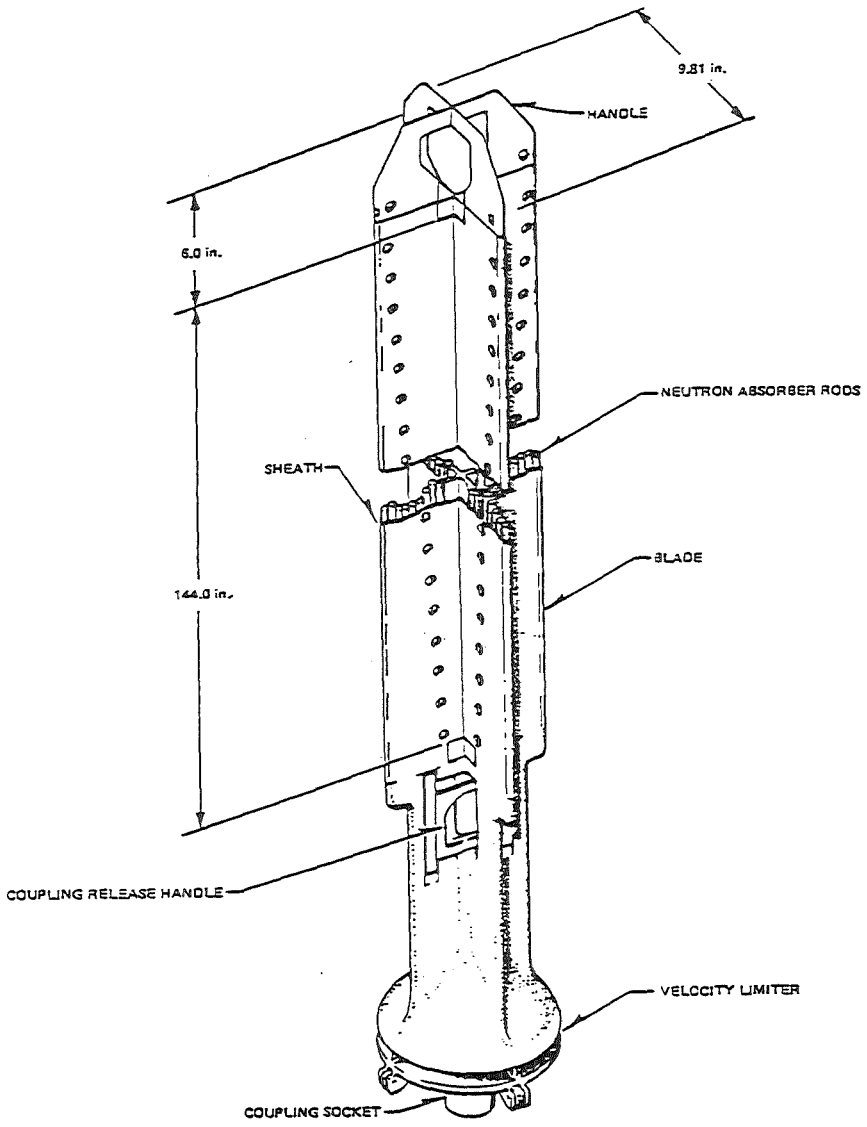

Fig. 20 BWR Control Rod Assembly.

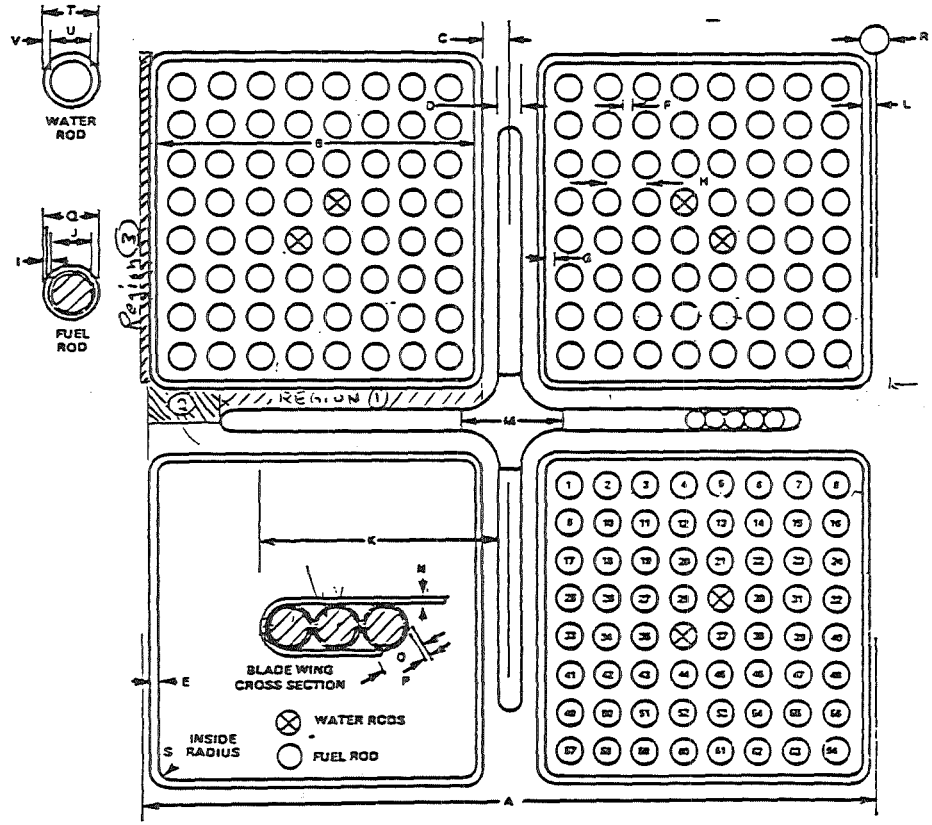

Inner diameter : 3.5mm = 0.14inch
THICKNESS TUBE : 0.64mm = 0.025inch
THICKNESS BLADE : 1.42mm = 0.056inch
DISTANCE BETWEEN BOXES : 18mm = 0.71inch

Fig. 21
Cross section of BWR control rod inside fuel element.

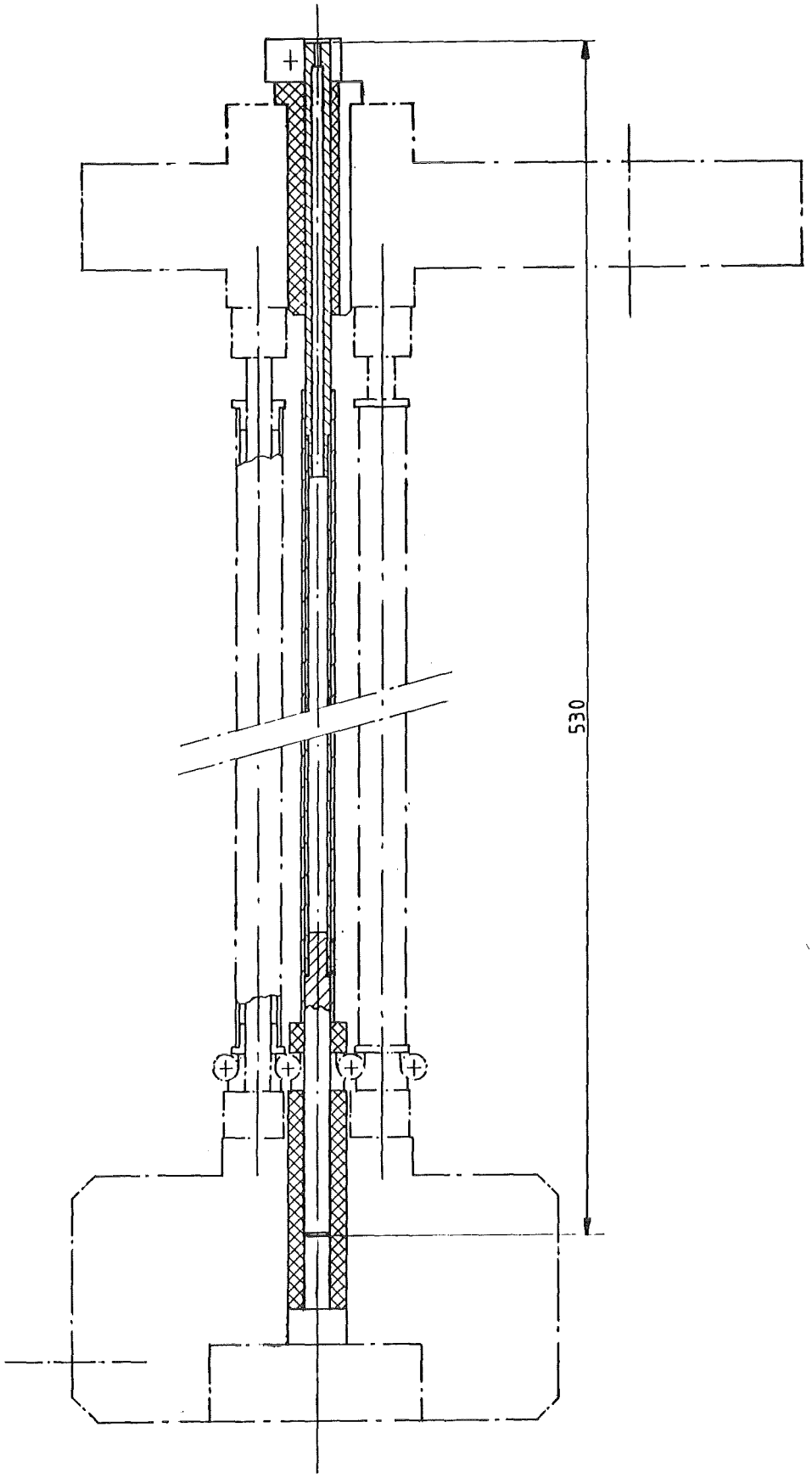

Fig. 22
B_4C-absorber test arrangement (B1)

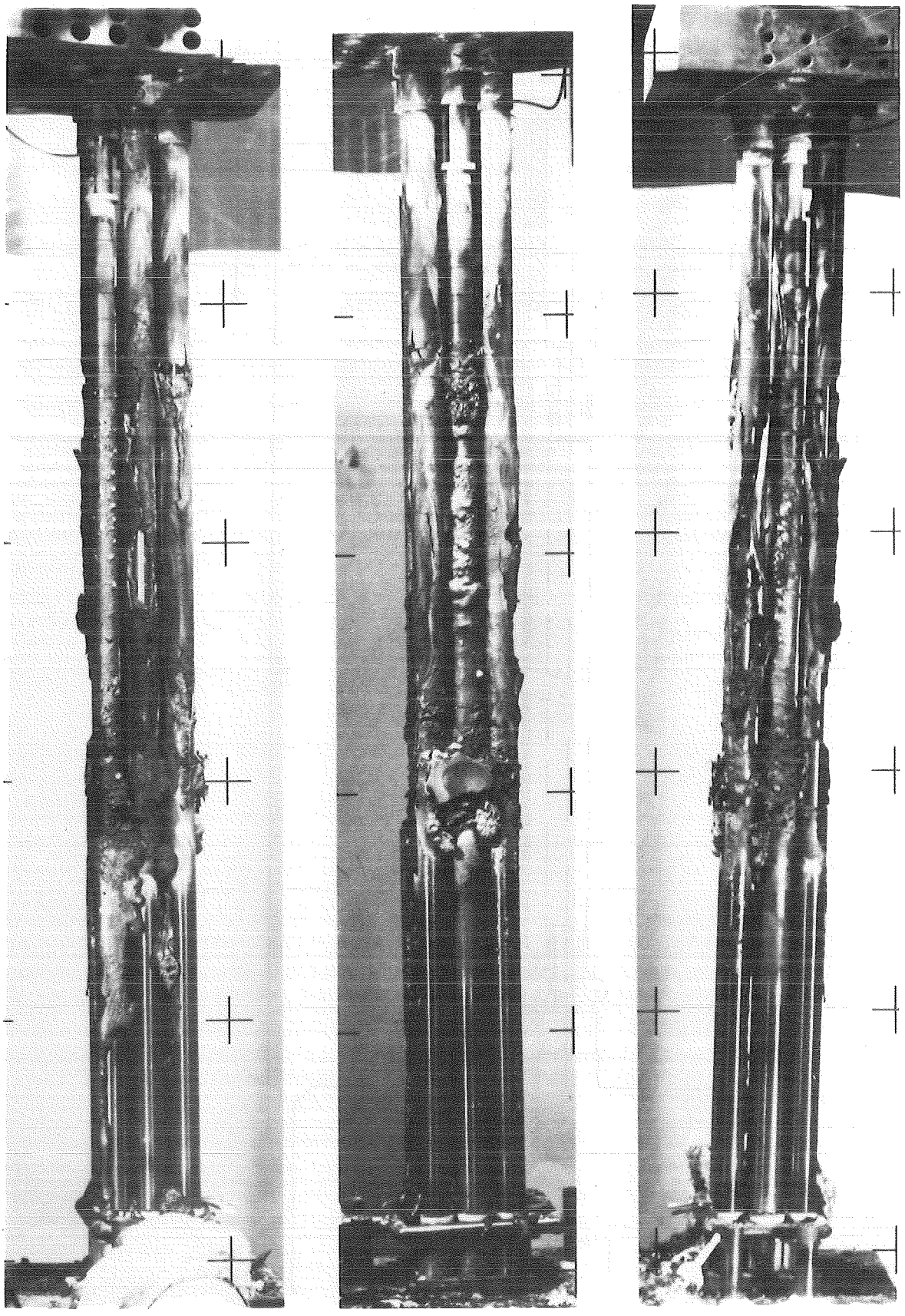

Fig. 23: Post test appearance of bundle B1 seen from different directions.

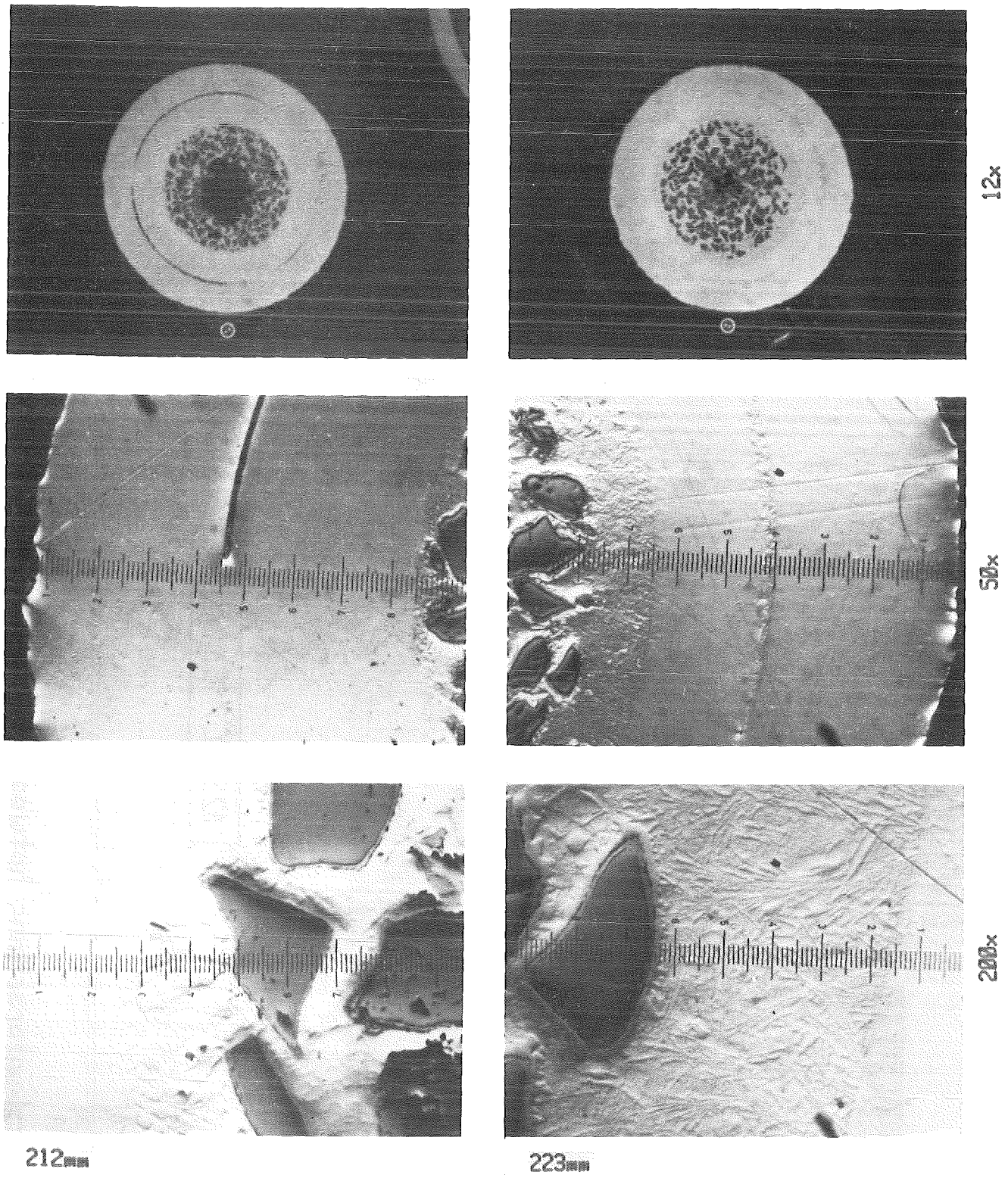

Fig. 24: Details of absorber rod cross section at 212 mm and 223 mm elevation (B_4C - test B2)

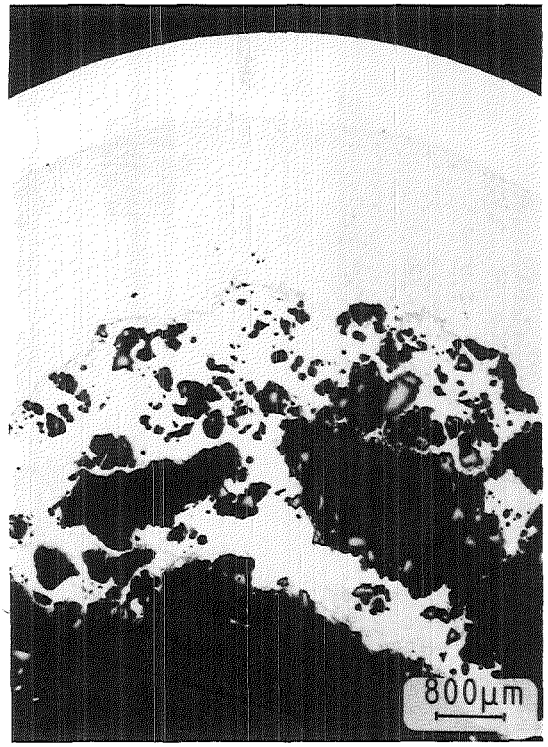

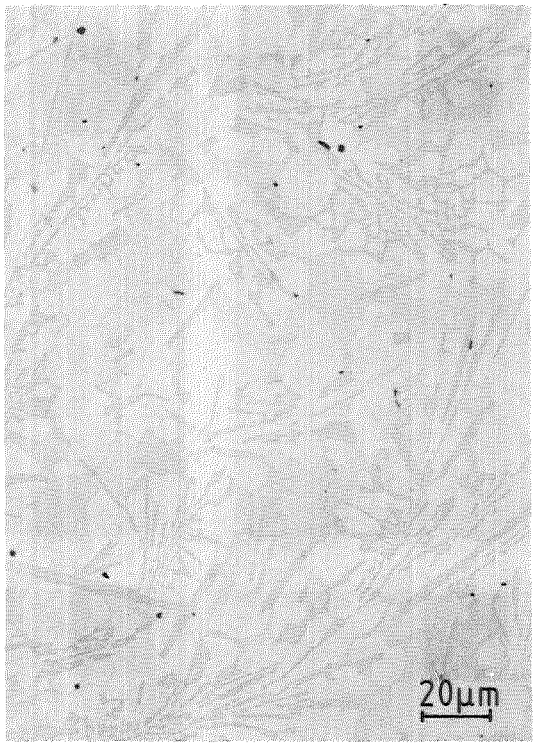

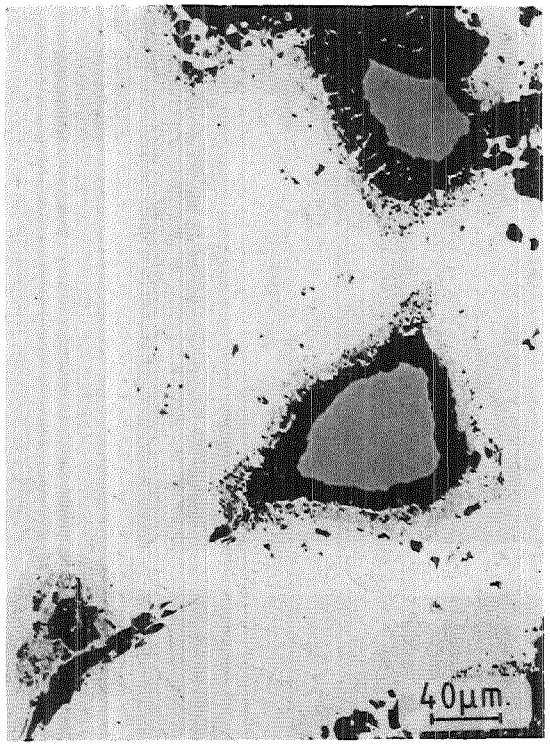

1230°C / 15 min

KfK IMF I

Fig. 25: Chemical interactions between B_4C and stainless steel type 316

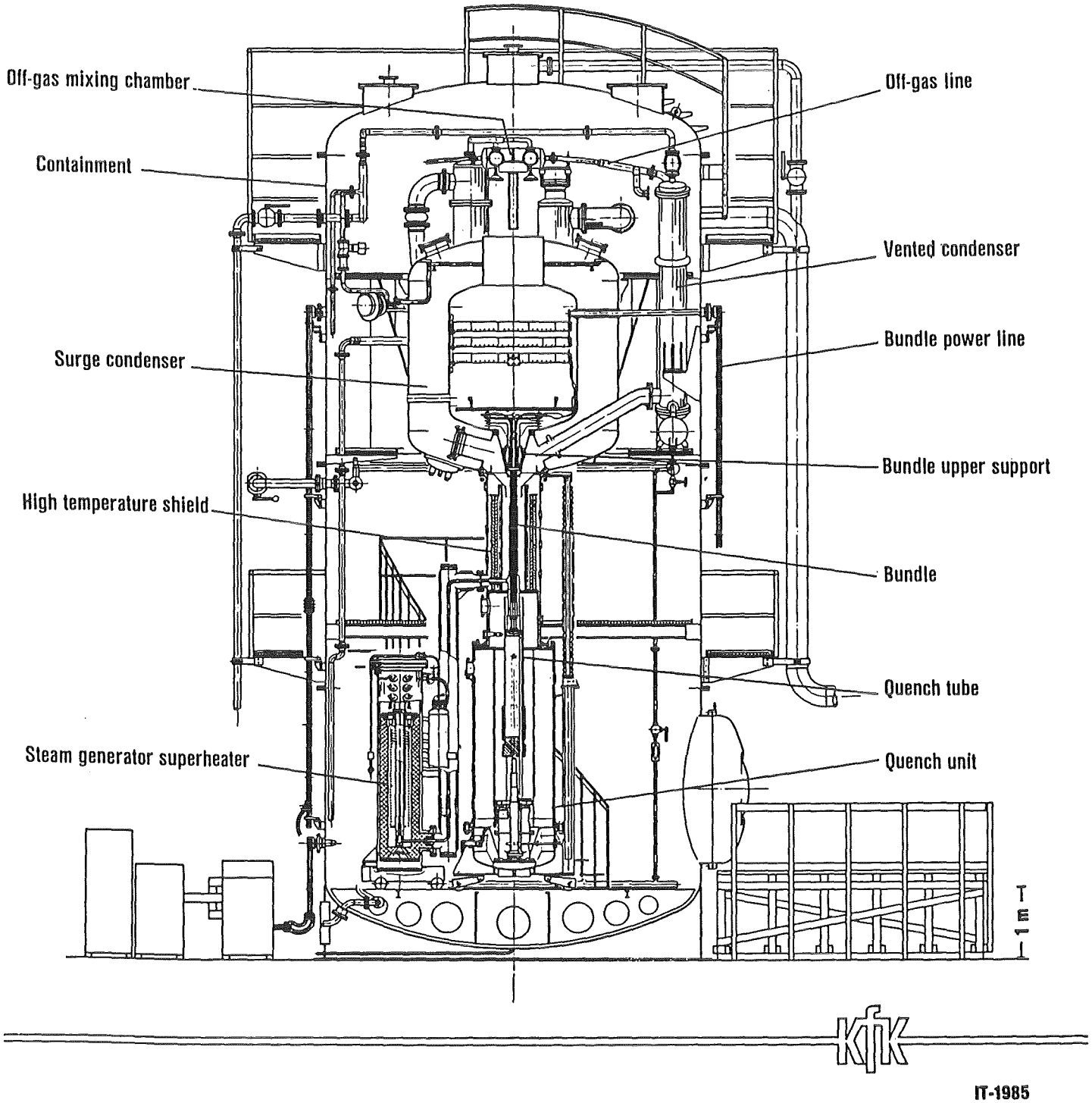

Fig. 26: SFD-Test Facility CORA

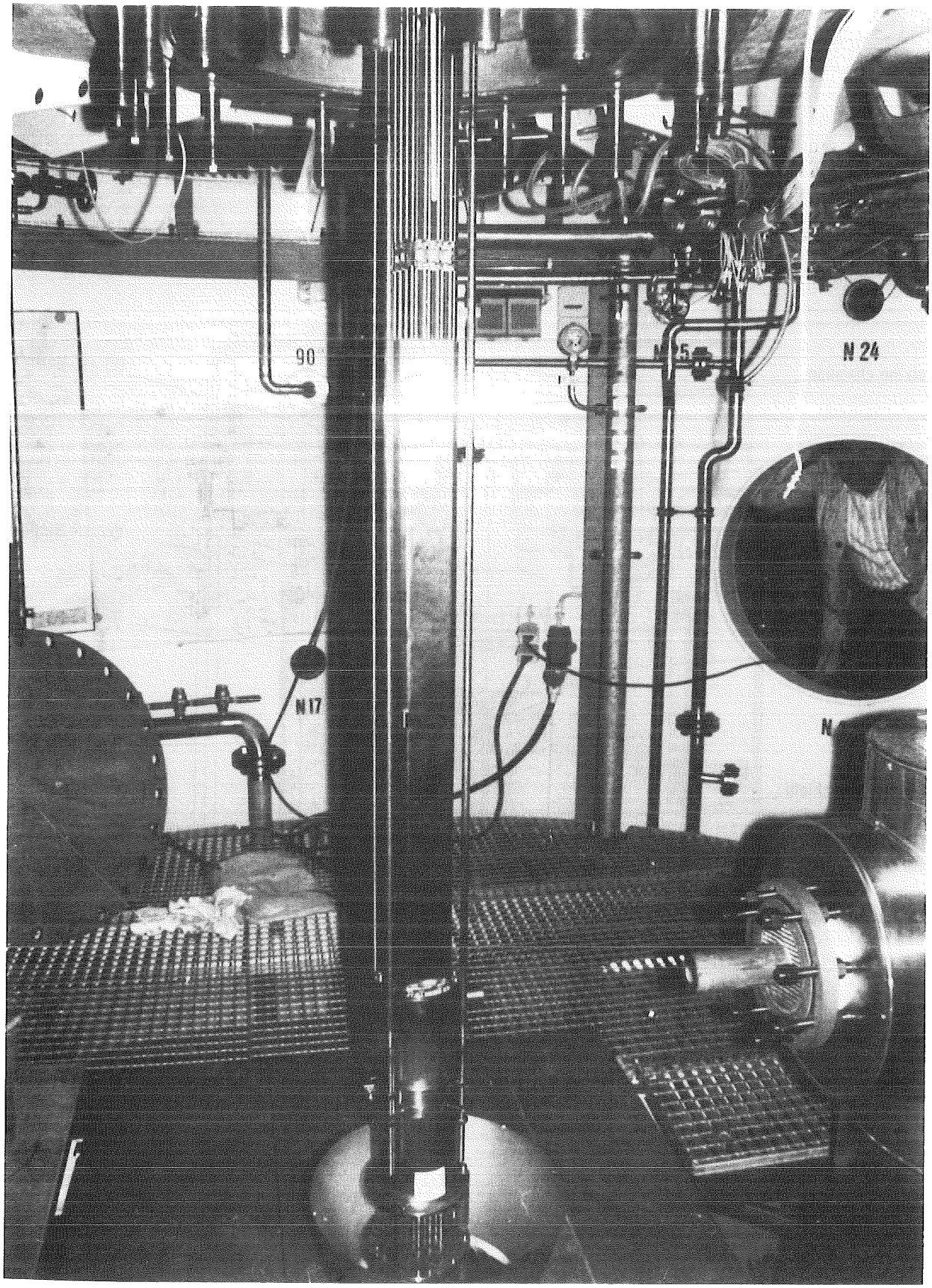

Fig. 27: CORA-bundle before test, the high temperature shield is lowered into the quenchtank

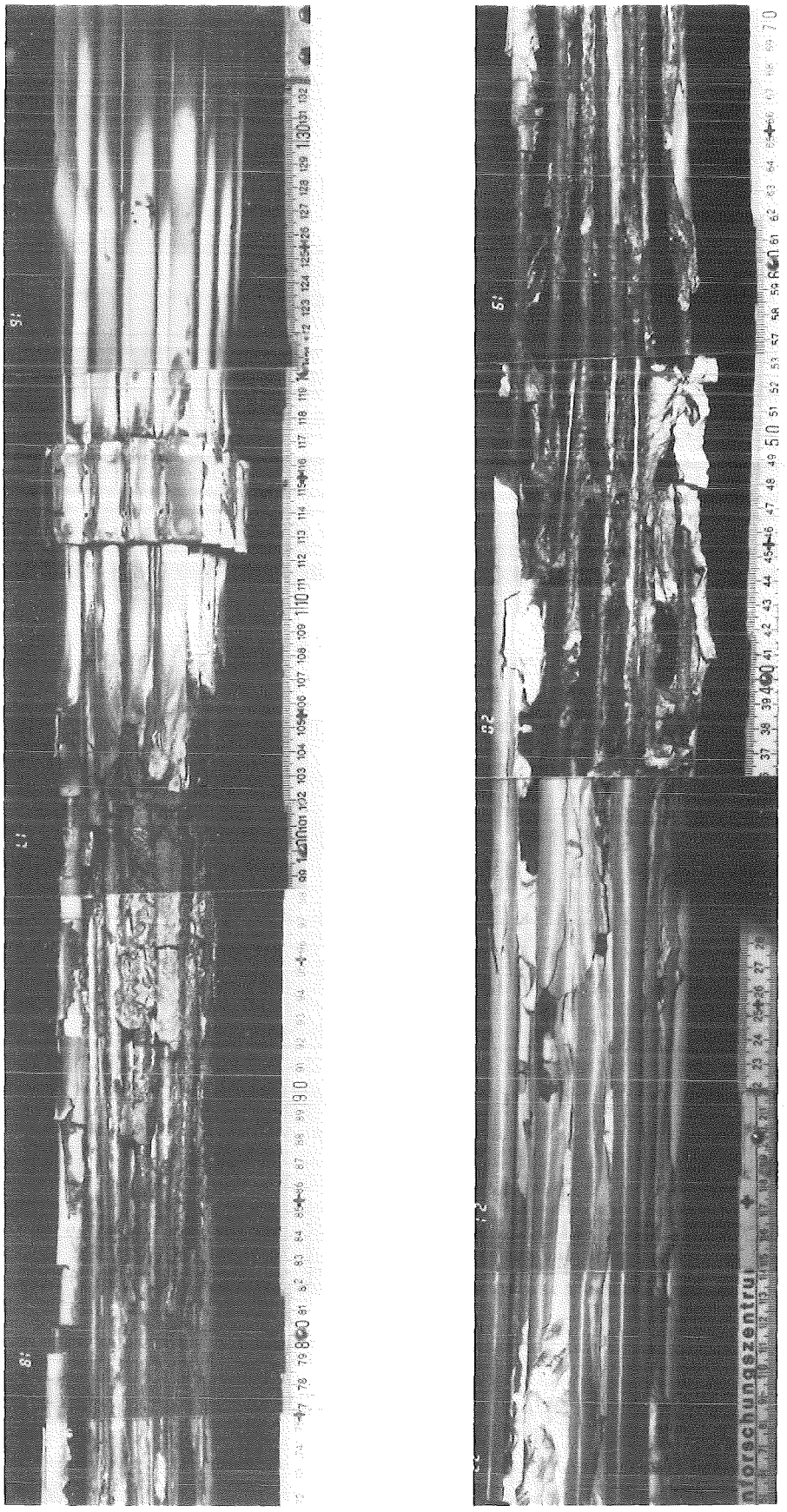

Fig. 28: Posttest view of the bundle CORA scoping test B (Al_2O_3 pellets)

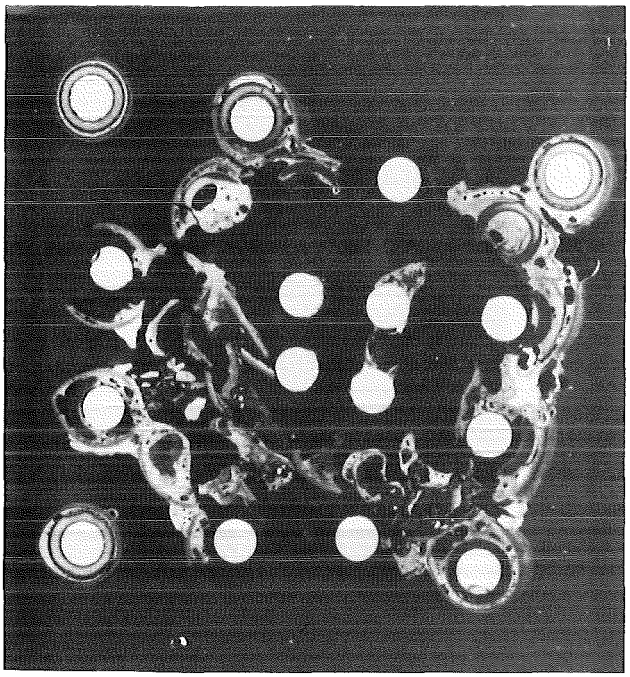

269 mm

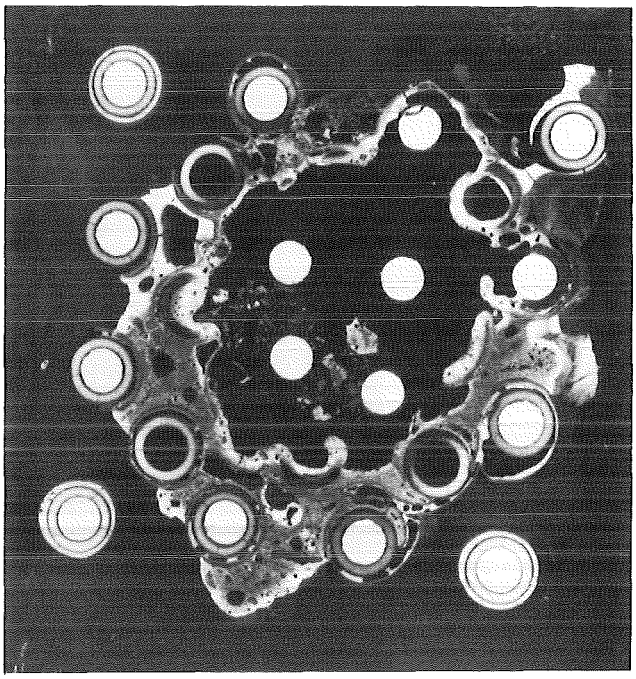

91 mm

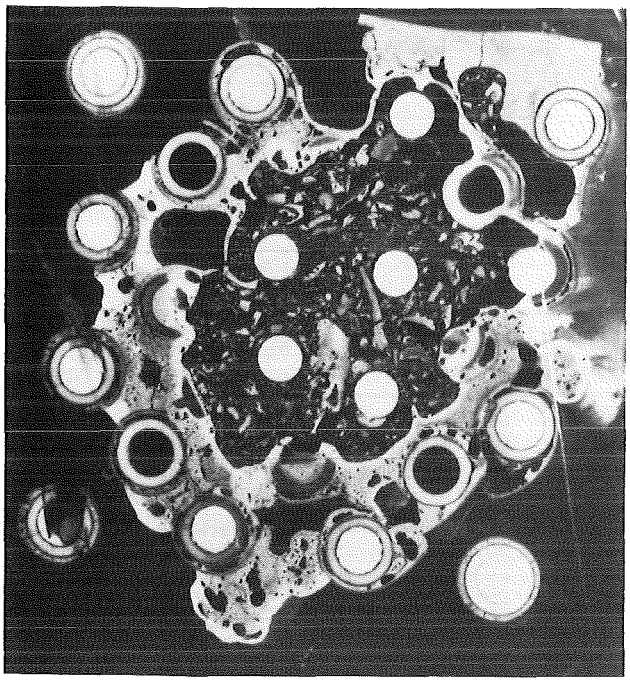

73 mm

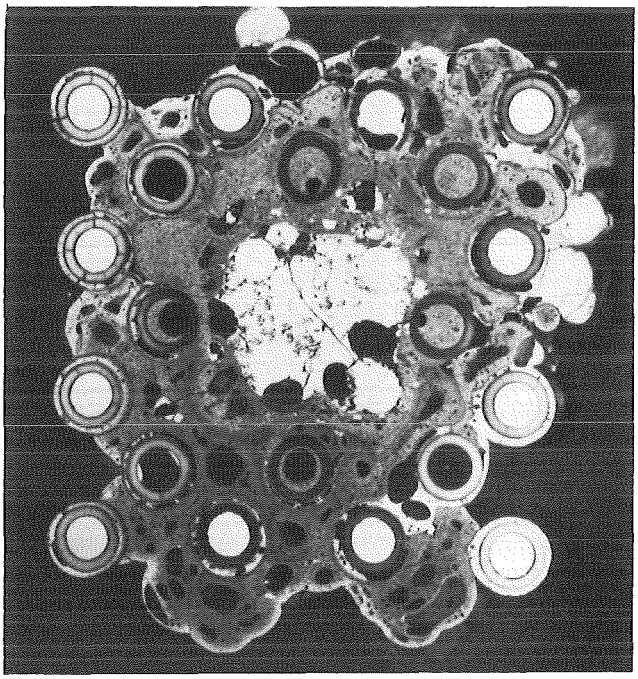

Ø mm

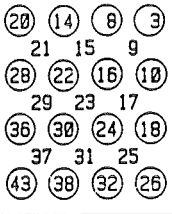

Fig. 29 : Cross sections of CORA bundle B at elevations given (bundle code)

Test No.	Cladding Temperature [°C]	System atmosphere	System pressure [bar]	Rod pressure [bar]	Ballooning and bursting	Test termination	Bundle configuration	Absorber/ Guide tube	Test objectives, remarks
1	< 1850	argon	1	1	none	cooldown in argon	type a	No / No	Scoping test, heat transfer calibration
2	1850	steam-	1	1	none	argon purge	type a	No / No	reference test w/o. absorber material
3	2400	starved	1	1	none	argon purge	type a	No / No	reference test w/o. absorber material
4	> 1200	"	1	1	none	argon purge	type a	1-Ag In Cd / Zry	control rod failure at low system pressure
5	1850	"	1	1	none	argon purge	type a	1-Ag In Cd / Zry	Zry clad melting
6	2400	"	1	1	none	argon purge	type a	1-Ag In Cd / Zry	extensive fuel liquefaction (monotect ic melting)
7	2400	"	1	1	none	argon purge	type c	4-Ag In Cd / Zry	different bundle configuration
8	> 1200	"	10	1	none	argon purge	type a	1-Ag In Cd / Zry	control rod failure at elevated system
9	2400	"	10	1	none	argon purge	type a	1-Ag In Cd / Zry	pressure, to be compared with test 4 + test 6
10	2400	steam rich	1	1	none	argon purge	type a	1-Ag In Cd / Zry	influence of steam supply, to be compared with Test 6
11	> 1200	steam-	1	1	none	quench	type a	1-Ag In Cd / Zry	influence of quenching, to be compared with Test 4
12	1850	starved	1	1	none	quench	type a	1-Ag In Cd / Zry	influence of quenching, to be compared with Test 5
13	2400	"	1	1	none	quench	type a	1-Ag In Cd / Zry	influence of quenching, to be compared with Test 6
14	> 1350	"	1	1	none	argon purge	type a	1-Ag In Cd / SS	behaviour of SS guide tube, to be compared with Test 4
15	[a]	"	1	[a]	yes	argon purge	type a	1-Ag In Cd / Zry	influence of internal rod pressure

[a] to be determined

Initial heating rate: 1 °C/s

State of pellets: as received

Fig. 30 : Test Matrix for Out-of-Pile Bundle Experiments on Severe Fuel Damage (CORA)